

## MSC ENGINEERING RESEARCH REPORT

---

# A STUDY OF THE INFLUENCE OF THE OUTER SEMICONDUCTING LAYER ON THE HIGH FREQUENCY CHARACTERISTICS OF MV POWER CABLES

Gianpaolo Antonio Franco Mariano

A research report submitted to the Faculty of Engineering and the Built Environment, University of the Witwatersrand, Johannesburg, in partial fulfilment of the requirements for the degree of Master of Science in Engineering.

Johannesburg, 2015

# DECLARATION

I declare that this research report is my own unaided work except where specifically acknowledged. It is being submitted in partial fulfilment of the requirements for the Degree of Master of Science in Engineering to the University of the Witwatersrand, Johannesburg. It has not previously been submitted for any degree or examination to any other university.

---

Gianpaolo Antonio Franco Mariano

---

Date

# ABSTRACT

Advancements in smart grid technology have created a need for reliable forms of data transmission to be able to provide the various intelligent features associated with smart grids. One means of data transmission is Power Line Communication (PLC), which transmits data via the power cable with the cable simultaneously performing its normal function of carrying electric power. This is made possible by using suitable coupling interfaces. Attenuation, phase constant and propagation velocity are important characteristics of High Frequency (HF) signal transmission that need to be considered when understanding a power cable's data transmission capability. This research report investigates the extent to which the outer semiconducting layer of an Medium Voltage (MV) power cable affects the HF transmission characteristics by quantifying and comparing HF characteristics. Simulations were performed based on an established HF cable model. The simulations indicated that the outer semiconducting layer has an effect, although marginal, on the HF characteristics. The mean difference of attenuation between 1 to 10 MHz is  $2.849 \times 10^4$  db/m (3.08%). In the same frequency range the mean difference between the phase constant is 3.82% and the propagation velocity is 4.2%. Physical experimentation was carried out using a Time Domain Reflectometry (TDR) based measurement system. The resultant measurements further confirmed that the outer semiconducting layer has an influence on the HF transmission characteristics of the power cable. Time domain analysis, showed that the outer semiconducting layer has an effect on the velocity factor of the cable with a difference of 5.15%. Frequency domain analysis showed that the mean attenuation difference for the range of 1 to 7 MHz was 0.0054 dB/m (1.14%), which is relatively small when compared to the

simulation value. The outer semiconducting layer has a greater influence on the phase constant and propagation velocity with mean differences of 31.11% and 41.18%, which are significantly larger when compared to the values obtained through simulations. It was also determined that the length of the cable has an effect on the attenuation and usable bandwidth of the power cable with a shift of the peak attenuation from 55 to 45 MHz. In comparing the power cable with a communication (RG-58) cable of the same length it was seen that the RG-58 was better suited for HF transmission within its designated bandwidth and further showed the limitations of PLC. Design of communication channels in MV power cables should take cognisance of the power cable HF transmission limitations caused by components such as the outer semiconducting layer.

*To my family,  
without whom I would not have made it.*

# ACKNOWLEDGEMENTS

The author would like to thank Prof. Cuthbert Nyamupangedengu for his continuous support and guidance, and for his inspiration, enthusiasm and insight.

# CONTENTS

<b>DECLARATION</b>	<b>i</b>
<b>ABSTRACT</b>	<b>ii</b>
<b>ACKNOWLEDGEMENTS</b>	<b>v</b>
<b>LIST OF FIGURES</b>	<b>viii</b>
<b>LIST OF TABLES</b>	<b>x</b>
<b>1 INTRODUCTION</b>	<b>1</b>
<b>2 BACKGROUND</b>	<b>4</b>
2.1 Introduction . . . . .	4
2.2 Time Domain Reflectometry (TDR) in cable fault detection and PD location . . . . .	4
2.3 Power Line Communication (PLC) . . . . .	7
2.4 MV Power Cable Structure . . . . .	9
2.5 High Frequency Characteristics of a Power Cable . . . . .	11
2.6 Conclusion . . . . .	16
<b>3 SIMULATIONS OF THE POWER CABLE HF RESPONSE</b>	<b>17</b>
3.1 Introduction . . . . .	17
3.2 The Cable Model . . . . .	18
3.3 Simulation Results . . . . .	18
3.4 Summary . . . . .	23

<b>4</b>	<b>PHYSICAL MEASUREMENTS OF POWER CABLE HF RESPONSE</b>	<b>24</b>
4.1	Introduction . . . . .	24
4.2	The Network Analyser Method . . . . .	25
4.3	The Chosen TDR Measurement Methodology . . . . .	27
4.4	Test Setup and Procedure . . . . .	30
4.5	Different Test Cases . . . . .	36
4.5.1	Comparative test of MV power cable of the same length with and without the outer semiconducting layer . . . . .	36
4.5.2	Comparative tests of MV power cables of different length . . . . .	37
4.5.3	Comparative test of MV power cable and a communication cable of the same length . . . . .	37
<b>5</b>	<b>EXPERIMENTATION RESULTS AND DISCUSSION</b>	<b>38</b>
5.1	Introduction . . . . .	38
5.2	Calibration of the TDR Method . . . . .	38
5.3	Time Domain Response . . . . .	40
5.4	Frequency Domain Response . . . . .	42
5.4.1	Attenuation . . . . .	43
5.4.2	Phase Constant . . . . .	47
5.4.3	Propagation Velocity . . . . .	49
5.5	Summary of Results . . . . .	50
5.6	Conclusion . . . . .	52
<b>6</b>	<b>CONCLUSION</b>	<b>54</b>
	<b>REFERENCES</b>	<b>56</b>
<b>A</b>	<b>Matlab<sup>®</sup> Code</b>	<b>60</b>
A.1	Simulation . . . . .	60
A.2	TDR Analysis . . . . .	66
A.2.1	Function Files . . . . .	66
A.2.2	Code Implementation . . . . .	69



# LIST OF FIGURES

2.1	Overview of Chapter . . . . .	5
2.2	Typical structure of a MV power cable . . . . .	10
2.3	High Frequency Power Cable Model . . . . .	12
3.1	Simulated attenuation constant of MV power cable with and without the outer semiconducting layer . . . . .	20
3.2	Simulated phase constant of MV power cable with and without the outer semiconducting layer . . . . .	21
3.3	Simulated propagation velocity of MV power cable with and without the outer semiconducting layer . . . . .	22
4.1	Two port S-parameter network . . . . .	26
4.2	Time domain measurement setup . . . . .	29
4.3	8.25 m 11 kV single core cable used in testing . . . . .	31
4.4	RIGOL DS6062 600 MHz Digital Oscilloscope . . . . .	31
4.5	Hewlett Packard 8002A Pulse Generator . . . . .	32
4.6	Mini Circuits Signal Splitter ZFRSC-2050 . . . . .	32
4.7	1 m communication (RG-58) cable segments . . . . .	33
4.8	TDR experimental setup . . . . .	33
4.9	TDR test procedure flow chart . . . . .	35
5.1	Time domain response of 8.25 m and 20 m power cable . . . . .	39
5.2	Time domain response of MV power cable and RG58 cable . . . . .	40
5.3	Time domain response of MV power cable with and without the outer semiconducting layer . . . . .	42

5.4	The change in attenuation of MV power cable with and without the outer semiconducting layer as a function of frequency .	44
5.5	The change in attenuation of 8 m and 20 m MV power cable as a function of frequency . . . . .	46
5.6	The change in attenuation of MV power cable and RG58 cable as a function of frequency . . . . .	46
5.7	The change of the phase constant of MV power cable with and without the outer semiconducting layer as a function of frequency . . . . .	48
5.8	The change of the phase constant of MV power cable and RG58 cable as a function of frequency . . . . .	48
5.9	The change of the propagation velocity of MV power cable with and without the outer semiconducting layer as a function of frequency . . . . .	49
5.10	The change of the propagation velocity of MV power cable and RG58 cable as a function of frequency . . . . .	50

# LIST OF TABLES

3.1	Complex permittivity for insulation screen at 25°C . . . . .	19
3.2	Complex permittivity for screen bed at 25°C . . . . .	19
3.3	Structure and dimensions of simulated cable . . . . .	19
5.1	Comparison of Simulated and Physical Results . . . . .	51
5.2	Comparison between Power Cable With and Without Outer Semiconducting Layer . . . . .	51
5.3	Comparison between Power Cable and RG-58 Cable . . . . .	52

# Chapter 1

## INTRODUCTION

Smart grid technologies rely on advanced forms of information, communication and control technology, with the intelligent features being dependent on a reliable form of data transmission [1]. One of the important needs for effective data transmission is connection between the power utility and end users. Instead of laying new telecommunication cables, to provide a channel for communication, the existing power cable network can be used. It would reduce costs dramatically, taking advantage of the fact that the power utilities own these resources and in urban area with high population densities, transmission networks are already well established. The use of power cables as a means of data transmission is termed Power Line Communication (PLC). However, PLC is not the only high frequency signal transfer technology used in power systems. As an example a method termed Time Domain Reflectometry (TDR), which is essentially a high frequency technique, is used in locating faults in power cable networks.

Unlike cables used for communication purposes, such as twisted pairs or coaxial cables, the power cable is a far more complex structure as it is designed to conduct high currents and withstand high electric fields. Furthermore, power cables are designed for electric power transmission at 50 or 60 Hz and not the high frequencies associated with data transmission [1]. Research has been done in determining the effects of each layer of the cable structure on the high frequency (HF) characteristics of MV power cables.

However, minimal work has been done on determining the effect of the outer semiconducting layer on these characteristics. The research question of this research report work is as follows:

*Considering that MV power cables are being used to transmit high frequency signals, to what extent does the outer semiconducting layer of a power cable affect its HF parameters?*

The research question seeks to identify the specific contribution of the cable outer semiconducting layer to the overall HF response, therefore confirming or disproving any influence by the outer semiconducting layer on the HF transmission characteristics in power cables and thus adding value to current literature. The structure of the research report is as follows:

*Chapter 2* discusses the background of the different existing high frequency communication techniques and methodologies, such as TDR and PLC, currently being used in MV power cables. A review of how HF signals are being used helps motivate the necessity to fully understand the effects of the power cable structure on these HF signals. This chapter also describes the basic structure of an MV power cable, detailing each layer. Furthermore, the chapter presents the HF analytical model of the power cable.

*Chapter 3* provides results and discusses simulated data, using current theoretical HF models in literature, on the effects of the outer semiconducting layer on transmission of HF signals. The information obtained from the simulated results provides a basis for the expected results during the physical testing process.

*Chapter 4* details the methodology used for the experimental testing procedure with specific reference to TDR. It provides the necessary equations used to extract the HF characteristics from the time domain measurements for the implementation of a detailed analysis. It further details how the test was setup, the testing procedure and the different test scenarios implemented.

*Chapter 5* presents detailed analysis of data acquired during the TDR testing process, with emphasis on quantifying the effects of the outer semi-

conducting layer on the transmission of HF signals via MV power cables. Further analysis is carried on the cable length and the cable type comparison tests.

*Chapter 6* provides a conclusion on the findings of this research report.

*Appendix A* provides the Matlab<sup>®</sup> code that was used to simulate the HF characteristics and to analyse the TDR measurement.

# Chapter 2

## BACKGROUND

### 2.1 Introduction

This chapter discusses the background of the different existing high frequency communication techniques and methodologies, such as TDR and PLC, currently being used in MV power cables. A review of how HF signals are being used helps motivate the necessity to fully understand the effects of the power cable structure on these HF signals. The chapter also describes the basic structure of an MV power cable, detailing each layer. Furthermore, the chapter presents the HF analytical model of the power cable. *Figure 2.1* gives a schematic overview of the chapter.

### 2.2 Time Domain Reflectometry (TDR) in cable fault detection and PD location

Shielded power cables are vital components within the electrical distribution system. During operation, malfunctions such as open or short circuits may occur. Fault detection is important as it enables corrective measures to be taken to remove the problem from the system [2] and to restore effective operation.

When faults do occur on the power cable, there are protection systems in place that switch off the affected cable from the circuit. The fault on

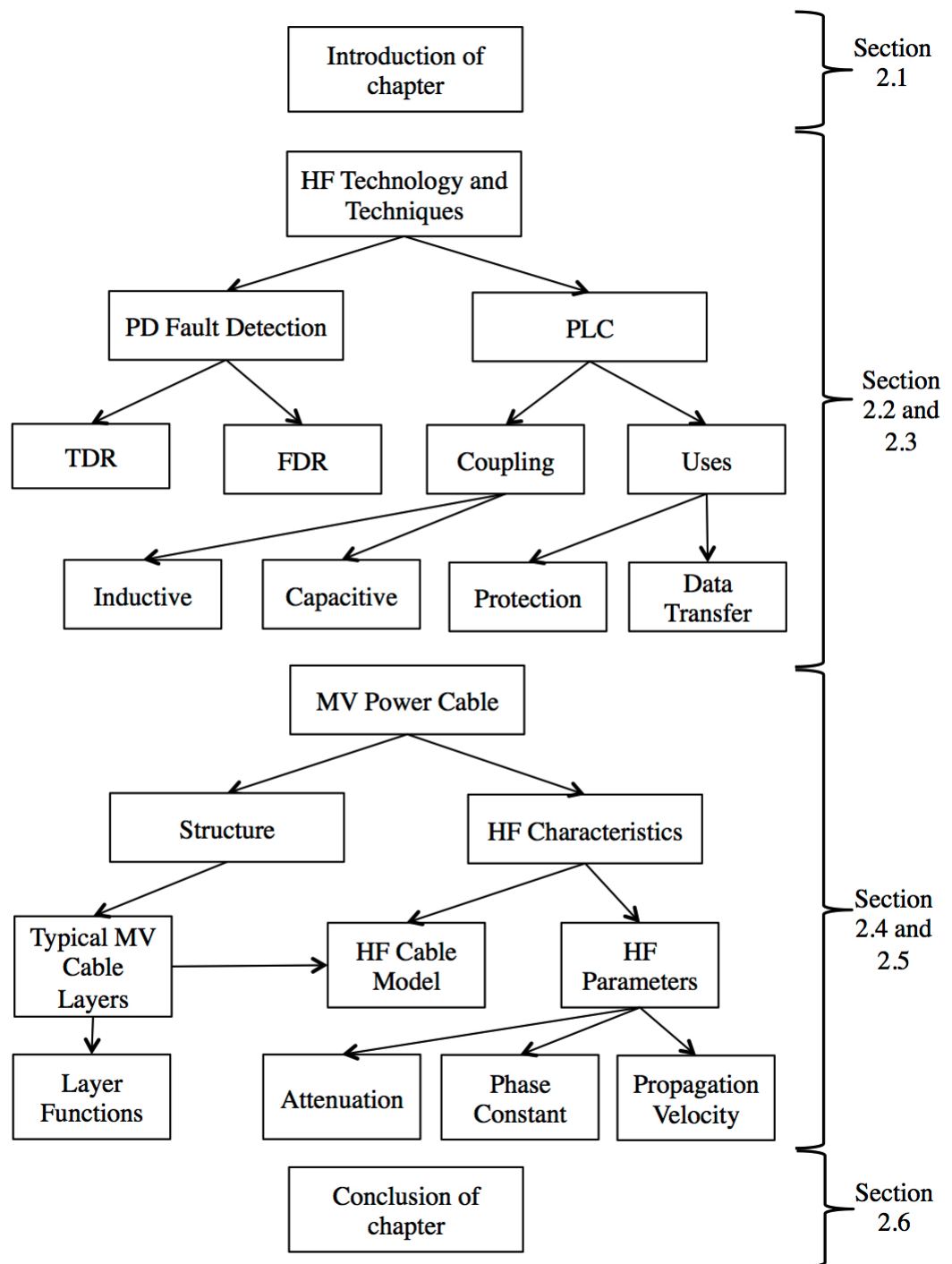


Figure 2.1: Overview of Chapter



the cable then needs to be identified and located so that maintenance can be carried out to restore power flow within the network. In most instances, power cables are buried and therefore the portion of the cable that contains the fault needs to be located precisely before digging up [2].

The incipient defects, which are commonly associated with partial discharge (PD), that cause the fault, are often due to ageing or degradation or are found in the cable accessories such as joints and terminations [2].

Time domain reflectometry is an important technique used in cable fault detection. TDR makes use of sending a short rise time pulse down the power cable and analysing the reflections caused by the impulse. The location of the fault in a cable can be obtained by making use of the propagation velocity and pulse travel time. These times are deduced from either time of arrival or time of flight difference. This method detects the change of impedance due to the fault.

Making use of the same principle as TDR or the frequency domain reflectometry (FDR), PD sources can be located. This technique is commercially used and is often referred to as PD mapping [3–5].

Travelling wave based measurements systems used in PD source location use either one or both ends of the cable [3]. Using only one end of the cable, a single instrument is used to receive a first pulse which propagates directly from the PD location to the end of the cable. A second pulse, which is a result of reflection off the opposite end of the cable, is received later [3, 4]. This type of measurement configuration is most commonly used in PD source location.

In the second configuration of using both cable ends, the PD-induced pulse is detected at both ends of the cable [3]. In this configuration, the time between the two pulses is used to determine the location of the PD. Furthermore, a calibration procedure of injecting a pulse at one end of the cable is used to determine the total propagation time of the cable under test [3].

Errors in PD location are caused by both electrical and mechanical phenomena. The electrical phenomena include: 1) Pulse distortion caused by frequency-dependent propagation characteristics of a solid dielectric cable,

2) Time based errors and 3) Interfering noise caused by the circuit.

The attenuation of a power cable is a strong function of frequency. This is due to the different dielectric layers within its structure. The very high frequency components of the pulse are lost very quickly as the pulse travels along the cable, while the lower frequency components are more stable [3]. This causes a problem in accurately determining PD location.

As mentioned above, fault detection is a precise exercise and therefore, it is important to know the cable's high frequency characteristics in order to achieve greater accuracy in determining the position of a fault within a power cable. In order to provide the accuracy needed, it is important to understand how the cable structure influences the detection and location methods, and further understanding the influence of the outer semiconducting layer.

## **2.3 Power Line Communication (PLC)**

There is a large variety of communication technologies that can be used in the physical realisation of smart grid infrastructures, with each having its own advantages and disadvantages. Technologies include: wire lines and fibre-optic cables, wireless communication (GPRS, GSM, WiMax etc.), radio communication and wireless local area networks (WLAN, WiFi, etc.) and PLC [6, 7].

Cost is an important factor to consider in the physical implementation of such technologies. Among all the options listed above, PLC is the only wire line based technology that has a relative cost, which is comparable to wireless setups. This is due to the fact that the cables are already installed, and it will have no service cost. Therefore it is highly important to fully investigate PLC technology and to determine ways to deal with its limitations [6].

The technology of superimposing high frequency signals on conducting power cables is fairly mature [8]. In 1995 it was shown that low voltage (LV) power cables could be used as a means of carrying high frequency signals (>1 MHz), that brought about the concept of broadband PLC [9]. Even though LV and Medium Voltage (MV) cables differ in design and structure, the principle of HF signal transmission is the same, and thus there is a

possibility of using MV cables as a channel for HF transmission.

An important aspect of PLC is the coupling of the communication signal onto the power line. The circuits used for power transmission and for communication act independently, and these different circuits have to be coupled by a coupling interface in order for PLC to work [10].

There are two possible methods of coupling the communication signal onto a power line: capacitive coupling interface or inductive coupling interface.

Firstly, the capacitive coupling interface is used in low voltage applications [10] therefore is not detailed further.

Secondly, the inductive coupling interface is used in MV applications. The interface components are connected in series with the electric loads. The main application for the interface is in broadband communication in HF band in power distribution grids [10]. The typical broadband bandwidth is between 1.8 to 30 MHz [11]. The supply line current magnetises the core materials within the inductive coupling interface, due to the serial communication. Thus, the interface needs to be designed according to the maximum current to avoid core saturation [10].

PLC has often been used in relaying cable protection signals between the connecting substations; a technique termed teleprotection. This technology does not use sophisticated transmission techniques such as communication channels. Pavlidou, *et al*, [12] details the various communications techniques, such as modulation, coding and control, that need to be considered when more advanced transmission techniques are to be transmitted via power cables. With advances in such areas, power cables may be used as a channel for other communication signals such as voice, SCADA (system control and data acquisition) signals and PLC systems [2, 6].

The effects that can cause error in PD source location as mentioned in *Section 2.2* are the same considerations that need to be made for PLC as signal distortion will be problematic to successful data transmission. Therefore it is important to know the high frequency characteristics of the power cable as they affect the transmission of the data signal. A key area of this is understanding the effects of the dielectric layers (insulation layer and inner

and outer semiconducting layers) which are frequency dependent on the HF signal being transmitted. With knowledge in this area, useful compensations both in the hardware and software can be made to effectively implement PLC through the power distribution network.

In order to study the HF properties of a power cable, the construction structure of a typical MV power cable needs to be analysed as presented in the next section.

## 2.4 MV Power Cable Structure

A typical MV power cable is made of many layers of different material, each having a specific function to provide safe and efficient power distribution. The typical layers that are present in most cables are presented in *Figure 2.2* and are listed below [13]:

- Current carrying core (copper / aluminium);
- Inner semiconductor layer (conductor screen);
- Insulation layer;
- Outer semiconductor layer (insulation screen);
- Screen Bed;
- Metallic Screen; and
- Oversheath (polyethylene).

The *current carrying core* of the power cable is typically constructed from copper or aluminium with varying designs. The size of the core is based on the current-carrying capacity, short circuit current and voltage drop.

The *inner semiconducting layer* is constructed using semiconducting materials. The purpose of the layer is to ensure, firstly, that the electric field within the insulation is uniform and radial and secondly, that there is intimate contact between conductor and insulation.

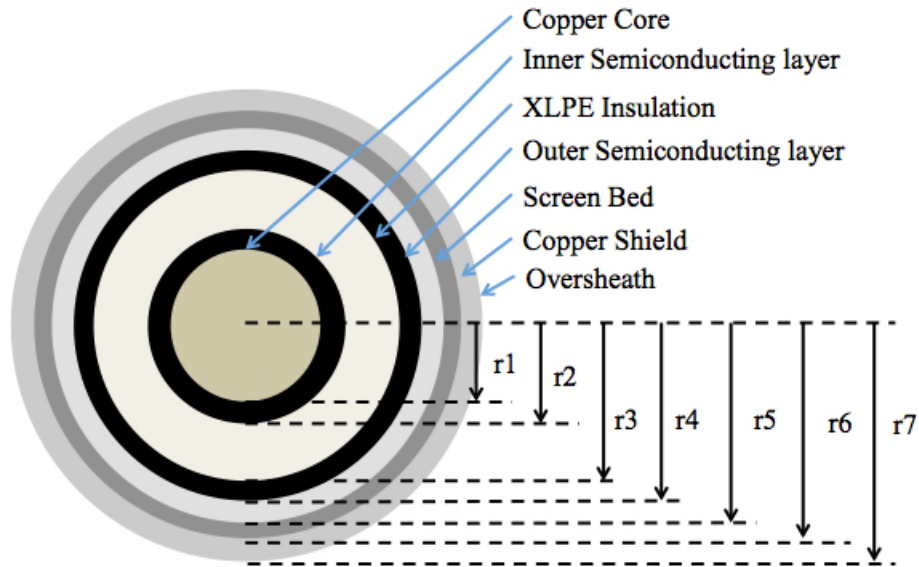


Figure 2.2: Typical structure of a MV power cable

The possibility of gaps and other deformation is reduced, which would cause irregularities in the electric field forming between the conductor and insulator.

The *insulation layer* is most commonly constructed with Cross-Linked Polyethylene (XLPE), however, in certain applications oil impregnated paper insulation is used. This layer is of the highest importance as it holds many vital functions for the cable's success. The insulation layer serves as a barrier to withstand the large potential difference between the core and the metallic shield, as result of the applied voltage. The insulation layer also functions to add mechanical reinforcement to the cable.

The *outer semiconducting layer* is constructed from the same material and has a similar function to that of the inner semiconducting layer; contributing to the electric field containment and ensuring a smooth interface between the insulation and metallic screen.

The *screen bed* is an inner sheath used to insure that the previous layers stay compact and together, and further provides a bedding for the metallic

screen (shield). This layer is typically constructed using a thermoplastic or thermosetting compound.

The *metallic screen (shield)* is constructed with either metallic tape or wire. It has the function of containing the electric field within the cable and also functions as the return path of current in single phase circuits.

The *oversheath* is used to protect the cable from adverse environment factors.

Variations in the structure of a power cable may occur due specific performance requirements. For example, cables that may be exposed to water will have a water blocking tape present within the structure to ensure no water will reach the inner layers.

It is important to note that power cables are designed for high voltage 50 Hz transmission, and each layer is designed to deal with the electric fields associated with such conditions.

For the power cable to function as a communication channel, the HF properties of the cable material and structure become important as analysed in the next section.

## 2.5 High Frequency Characteristics of a Power Cable

The high frequency equivalent circuit of a typical coaxial power cable is given in *Figure 2.3* [13].

The high frequency characteristics of a power cable are a combination of series impedances and shunt admittances. Series impedances ( $Z$ ) are due to the current carrying metallic core, and the metallic sheath. The series impedance of a cable is affected by a number of factors, firstly, the type of material used for the core and the metallic sheath, and secondly, the type of metallic sheath used, that is, either tape or strands. The shunt admittance ( $Y$ ) is due to the different material layers of the cable with each layer providing a loss ( $G_1$  to  $G_5$ ) and capacitance ( $C_1$  to  $C_5$ ) within the high frequency model as shown in *Figure 2.3*.

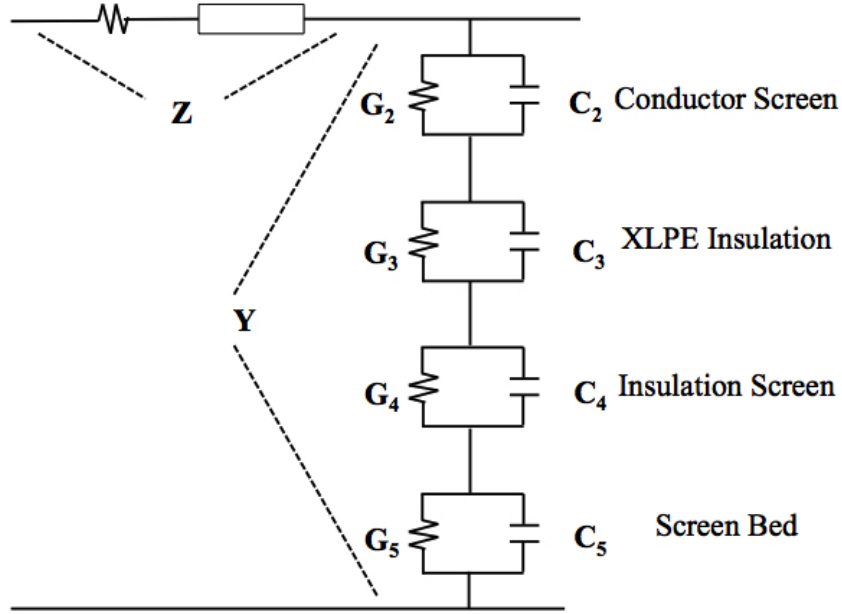


Figure 2.3: High Frequency Power Cable Model

The metallic shield has a major effect on the series impedance of the cable, therefore the formula used in determining the series impedance differs with each shield type. For a cable with a copper tape metallic shield, the series impedance,  $Z_T$ , is given in *Equation (2.1)* [14].

In the case of a cable that has an outer metallic shield made of  $N$  number of copper strands, with each strand having a radius of  $r_s$ , the series impedance,  $Z_S$ , for the cable is given by *Equation (2.2)* [15].

$$Z_T = \frac{1}{2\pi r_1} \sqrt{\frac{j\omega\mu_0}{\sigma_1(T)}} + \frac{j\omega\mu_0}{2\pi} \ln\left(\frac{r_5}{r_1}\right) + \frac{1}{2\pi r_5} \sqrt{\frac{j\omega\mu_0}{\sigma_6(T)}} \quad (2.1)$$

$$Z_S = \frac{1}{2\pi r_1} \sqrt{\frac{j\omega\mu_0}{\sigma_1(T)}} + \frac{j\omega\mu_0}{2\pi} \ln\left(\frac{r_5}{r_1}\right) + \frac{1}{2\pi N r_s} \sqrt{\frac{j\omega\mu_0}{\sigma_6(T)}} \quad (2.2)$$

$$\sigma_1(T) = \sigma_6(T) = \frac{1}{\rho(T)} = \frac{1}{\rho_0[1+\varphi(T-T_0)]} \quad (2.3)$$

Where, with reference to *Figures 2.2* and *2.3*:

$r_1$  and  $r_5$  are the radii of the core and the metallic sheath respectively

$\sigma_1(T)$  is the metallic core conductivity which is a function of temperature

$\sigma_6(T)$  is the metallic shield conductivity which is also a function of temperature

$\omega$  is the frequency

$\mu_0 = 4\pi \times 10^{-7}$  H/m. This is the permeability of free space

$\rho(T)$  is the resistivity

$\varphi = 3.862 \times 10^{-3}$  ° C is the temperature coefficient

$T_0 = 20$ ° C, the assumed ambient temperature.

Often the semiconducting layer has been treated as part of the conductor. The semiconducting layer however has a far greater resistivity value which is a function of frequency compared with that of the conductor and therefore must be treated as its own entity. This is due to the fact that the semiconducting layer is a composite of an insulation material containing carbon [16]. It is important therefore to determine the impedance and admittance of this layer separately from the conducting layer and the main insulation layer.

Work has been done in developing equations to quantify the series impedance and shunt admittance values for all layers of the cable [16].

In the development of the equations, Ametani [16] found that the effect of the semiconducting layer on the propagation constant is dominated by the admittance of the layer and not by the impedance. This was observed when the thickness of the layer is relatively small and the resistivity is high.

The total dielectric loss is a composition of the inner semiconductor layer, the insulation layer, the outer semiconductor layer and the screen bed. Each layer has a conductance value and most importantly is a lossy capacitor



which is frequency dependent. Thus with changes in frequency the respective conductance values will change as reported in Mugala (2005) [13].

The admittance of each layer of the power cable is the composition of the conductance value and the capacitance.

$$Y = \frac{1}{\sum \frac{1}{Y_k}} \quad (2.4)$$

$$Y_k = G_k + j\omega C_k = j \frac{\omega \pi \varepsilon_0 \varepsilon_k^*(\omega)}{\ln \left( \frac{r_k}{r_{k-1}} \right)} \quad (2.5)$$

Where:

$k$  is the number of the layer, i.e.  $k = 2, 3, 4, 5$ ;

$Y$  is the total cable admittance;

$Y_k$  is the admittance of the specific dielectric in the layer  $k$ ;

$G_k$  is the conductance of the specific dielectric in the layer  $k$ ;

$C_k$  is the capacitance of the specific dielectric in the layer  $k$ ;

$r_k$  and  $r_{k-1}$  correspond to the outer and inner radius, respectively, of the layer  $k$ .

In high frequency signal transmission, communication channels are typically characterised by the following parameters, which are extracted from the propagation constant ( $\gamma$ ):

- Attenuation of the signal ( $\alpha$ )
- Phase constant ( $\beta$ )
- Propagation velocity ( $v$ )

These characteristics are critical in understanding the effect of the cable on the quality of the signal transmission, as:

- Attenuation,  $\alpha$ , is the reduction of a signals strength per unit length. If a large amount of attenuation occurs on a signal, it will become

unreadable on the receiving end. Attenuation is important in most HF techniques.

- Phase constant,  $\beta$ , is important in telecommunication, and indeed PLC. It is the measure of the shift in phase of the signal as it travels a unit length. The phase constant is also often termed the wave number. The importance of the phase constant is in the use of phase modulation. With phase modulation it is important to have a detailed knowledge of the carrier signal, especially the phase of the signal and how it changes, so that the receiving end is able to handle the data being transmitted.
- The propagation velocity,  $v$ , allows for the calculation of the velocity factor of the cable, which compares the speed within the cable to the speed of light in a vacuum. This concept is explained further in *Section 5.3*.

By using *Equation (2.6)*, the values for HF characteristics can be determined if the  $Z$  and  $Y$  parameters are known as calculated from *Equations (2.1) or (2.2)*, and *(2.4)*.

$$\gamma(\omega) = \sqrt{ZY} = \alpha(\omega) + j\beta(\omega) \quad (2.6)$$

Further, Mugala (2005) [13] shows that the attenuation, phase constant, and velocity can be determined from the propagation constant,  $\gamma$ , using *Equations (2.7)*, *(2.8)* and *(2.9)*.

$$\alpha(\omega) = \text{Re}(Y(\omega)) \quad (2.7)$$

$$\beta(\omega) = \text{Im}(Y(\omega)) \quad (2.8)$$

$$v(\omega) = \frac{\omega}{\beta(\omega)} \quad (2.9)$$

The knowledge of the power cable HF parameters can therefore enable the determination of the cable HF response.

## **2.6 Conclusion**

The interest of smart grid technology and how it can provide better efficiency of power usage has brought with it increased research into the different components that make up a smart grid. In reviewing the various data transmission technologies providing communication between the various components of a smart grid, PLC is a prominent method. In this form of data transmission, the structure of the power cable has an effect on the response of the HF signal. With each layer contributing to the shunt admittance and cable series impedance, it is therefore important to know that each layer affects the attenuation, phase constant and propagation velocity of the HF signal. Significant research has been done on the effects of the various layers of the cable structure on HF transmission. However, the effects due to the outer semiconducting layer are not as yet fully known. The following chapters in the research report are focused on experimentally quantifying, and therefore confirming or disproving any influence by the outer semiconducting layer on the HF transmission characteristics in power cables.

The experimental study to address the research question entailed simulations and physical tests of the cable with and without the outer semiconducting layer as presented in the next chapter.

# Chapter 3

## SIMULATIONS OF THE POWER CABLE HF RESPONSE

### 3.1 Introduction

Before physical testing, the HF response of the MV power cable was simulated, using the HF cable model and the equations given in *Section 2.5*. Once the actual cable to be tested was identified, the necessary parameters for use in the simulation were determined, such as the cable dimensions and the complex permittivity values for the different insulation layers. In order for simulations to be successful, realistic values for the complex permittivity of the semiconducting material were obtained from Mugala [13], which provide the complex permittivities as a function of frequency. The HF parameters for the cable studied were then simulated. Comparative plots of the HF parameters with and without the outer semiconducting layer were produced, and a predicted influence of the outer semiconducting layer was determined.

The simulations provided a graphical representation of attenuation,  $\alpha(\omega, T)$ , phase constant,  $\beta(\omega, T)$  and propagation velocity,  $v(\omega, T)$ , where  $\omega$  is frequency and  $T$  is temperature. The analysis of the simulated results give a basis for the expected results obtained during the physical testing process.

## 3.2 The Cable Model

In *Section 2.5*, a theoretical model is described in detail, giving the equations for the series impedances and shunt admittances of the cable. Making use of this model and the equations, the HF response of a cable was simulated and the way in which HF signals are affected by the power cable structure was predicted. Additionally, the model was modified to simulate the cable without the outer semiconducting layer. A comparison was made between the frequency response of two models, thus determining the effect of the outer semiconducting layer on HF transmission.

The complex permittivity values for the insulation and the screen bed were taken from the graphs in Mugala (2005) [13] and Mugala, *et al.*, (2007) [14]. The complex permittivity of the XLPE insulation layer of the cable for all frequencies was assumed to be  $2.3 - j0.001$  [17]. *Tables 3.1* and *3.2* provide the permittivity values for the different layers of the cable at different frequency values as obtained from Mugala's work in [13, 14]. It must be noted that the same permittivity values were used for the inner and outer semiconducting layers. In the present work the cable available was an AXCE 7/12kV 1x95/25LT and therefore the resultant dimensions were adopted in the simulations. The dimensions of the cable used in the simulation are provided in *Table 3.3*, and referenced to the cable structure presented in *Figure 2.2*.

It must be noted that Mugala in [13], only provides permittivity values between 55 kHz and 550 MHz and therefore it was not possible to simulate the HF response of the cable for values lower or higher than that range.

## 3.3 Simulation Results

The model was implemented using Matlab<sup>®</sup> and the HF response characteristics were simulated. The parameters compiled included the attenuation, phase constant and propagation velocity of the cable for HF transmission. *Figures 3.1*, *3.2* and *3.3* show the difference between a power cable with and without the semiconducting layer present over a frequency range of

Table 3.1: Complex permittivity for insulation screen at 25°C

Frequency (MHz)	Real	Imaginary
1	130	18000
5.5	120	6000
10	110	1500
55	75	500
100	55	200
550	35	80

Table 3.2: Complex permittivity for screen bed at 25°C

Frequency (MHz)	Real	Imaginary
1	170	1500
5.5	125	350
10	75	150
55	50	60
100	35	26
550	25	15

Table 3.3: Structure and dimensions of simulated cable

Parameter	Length (mm)
$r_1$ - Conductor radius	6.75
$r_2$ - Inner Semiconducting Layer Thickness	1
$r_3$ - XLPE Insulation Thickness	3.25
$r_4$ - Outer Semiconducting Layer Thickness	1
$r_5$ - Screen Bed Thickness	1
Cable Length	8250

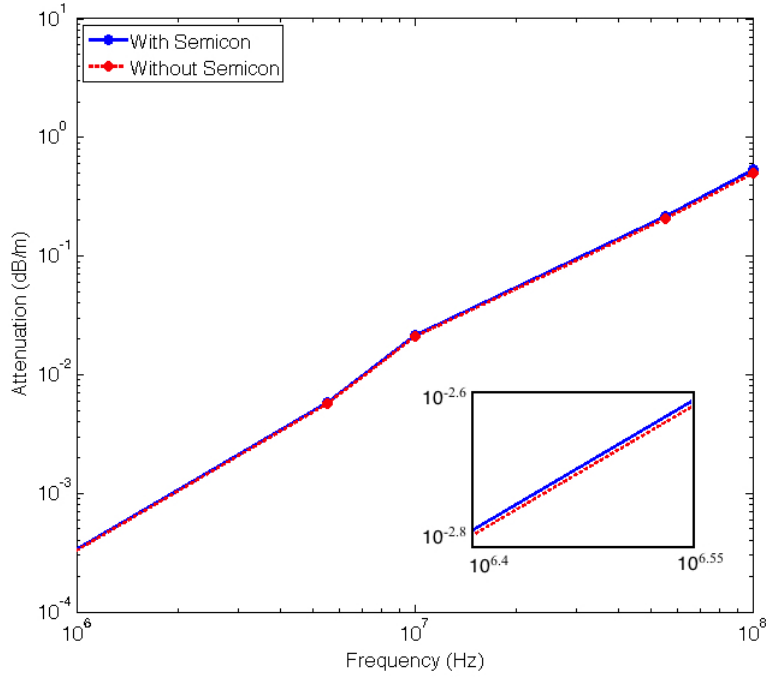


Figure 3.1: Simulated attenuation constant of MV power cable with and without the outer semiconducting layer

1 to 30 MHz. The code used in the simulation is provided in *Appendix A.1*.

In *Figure 3.1*, it is seen that the HF model of the power cable shows a linear relationship between the attenuation and the frequency, that is, attenuation increases with an increase in frequency. From 1 MHz to 100 MHz the attenuation value increases from  $3.4 \times 10^{-4}$  to 0.53 dB/m which is an increase of 1567%. The outer semiconducting layer increases the attenuation of the HF signal within the power cable. The power cable has a mean attenuation of 0.156 dB/m which reduces by an average of 6.41% in the frequency range of 1 to 100 MHz for the cable without the outer semiconducting layer. For the range of 1 to 10 MHz, the mean difference is  $2.849 \times 10^4$  dB/m (3.08%). Thus it can be deduced from the simulation results that the attenuation of the cable is influenced by the outer semiconducting layer. In comparing the results from this simulation and those by Ametani, *et al*, (2007) [16], it can be seen that the trend of the attenuation is similar for a cable with and without a semiconducting layer; the attenuation values increase with

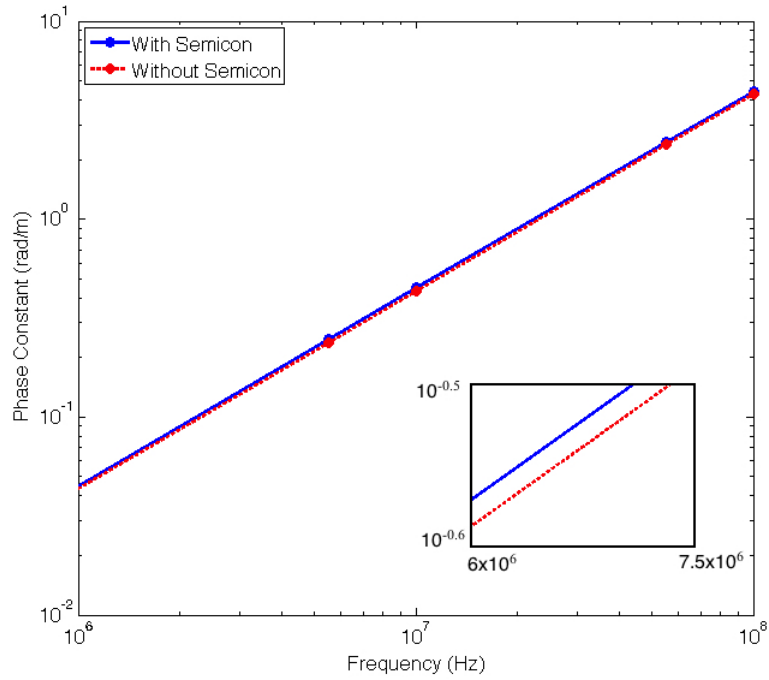


Figure 3.2: Simulated phase constant of MV power cable with and without the outer semiconducting layer

an increase in frequency. There is a difference however in the two cases of the actual attenuation values for both the power cable with and without the outer semiconducting layer. For the frequency range of 1 to 100 MHz, the simulation shows a greater increase in the attenuation values compared to Ametani, *et al*, (2007) [16].

The outer semiconducting layer increases the attenuation of the cable and therefore increase the loss of the signal strength over a given distance. This means that the outer semiconducting layer will reduce the quality of the HF signals being transferred over the MV power cable. As mentioned in *Section 2.5*, a large attenuation can cause the signal to become undetectable on the receiving end.

The simulated phase constant of the cable with and without the outer semiconducting layer is shown in *Figures 3.2*. It is evident that like the attenuation there is a linear relationship between the phase constant and frequency, and that the outer semiconducting layer increases the phase constant.



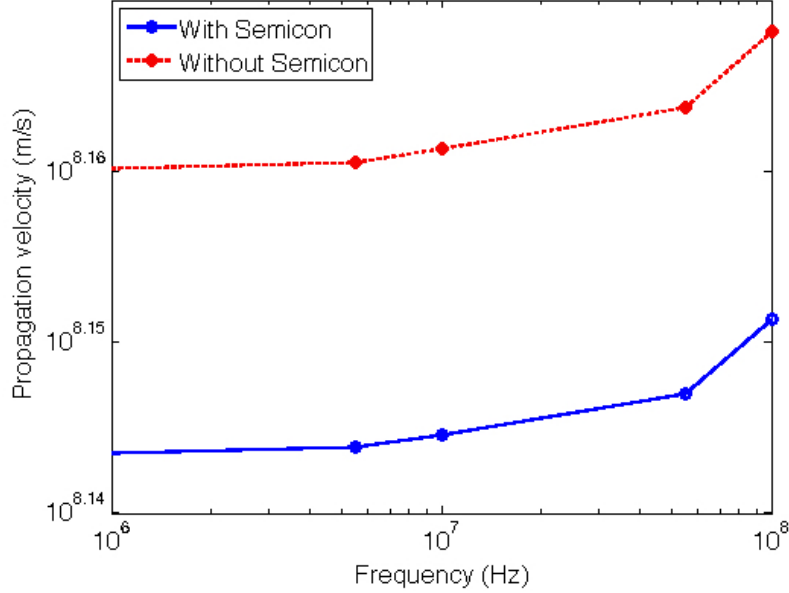


Figure 3.3: Simulated propagation velocity of MV power cable with and without the outer semiconducting layer

The mean phase constant for the power cable with the outer semiconducting layer was 1.52 rad/m and without the outer semiconducting layer showing a decrease of 4%.

A change in the phase constant will affect the characteristics of the waveform. As mentioned in *Section 2.5*, the importance of understanding the phase constant is when applying phase modulation to the signal. Therefore it is important to understand the characteristics of the signal.

With regard to the propagation velocity in *Figure 3.3*, it can be seen that the outer semiconducting layer has an effect on propagation velocity. The mean propagation velocity for the cable with the outer semiconducting layer was  $1.4 \times 10^8$  m/s and increased by an average of 4.2% when the outer semiconducting layer was removed.

The outer semiconducting layer decreases the propagation velocity of the HF signal being transferred. This reduction in turn means a delay in the HF signal from a point transmitting the signal to a point receiving the signal. A decrease in propagation velocity and velocity factor does not necessarily mean a reduction in the quality of the HF signal being transmitted but in cases where speed is a critical factor it can be an issue and there may be a loss in precision.

### **3.4 Summary**

The simulation results of the cable model based on Mugala (2005) [13] and Mugala, *et al*, (2007) [14], showed that for a range of 1 to 10 MHz, there is mean difference in the attenuation of the cable with and without the outer semiconducting layer of 3.08%. Furthermore, the mean differences of the phase constant and propagation velocity are 4% and 4.2% respectively. It can be concluded from the simulation results that the outer semiconducting layer has an effect on the HF characteristics of the 11 kV MV power cable. Physical experimental tests were performed to verify the simulation results as presented in the next chapter.

# Chapter 4

## PHYSICAL MEASUREMENTS OF POWER CABLE HF RESPONSE

### 4.1 Introduction

Physical measurements on the power cable HF response comprised of a testing procedure using a TDR based method whereby a pulse is transmitted down the cable and the reflections measured. The cable was kept open circuited on the far end. Using the time domain waveform produced by the reflections, the velocity of the pulse was determined, further allowing for the calculation of the velocity factor. The velocity factor was necessary to compute as it provided an analysis of the change in propagation velocity of the pulse and thus a comparison was made in each test scenario. After a time domain analysis and making use of the equations in Section 4.3, the frequency domain characteristics of the cable were determined. The characteristics included: the attenuation,  $\alpha(\omega, T)$ , phase constant,  $\beta(\omega, T)$ , and propagation velocity,  $v(\omega, T)$ . Using the HF characteristics, the following test scenarios were implemented:

- A comparison of the transmission characteristics between a typical power cable with and without the outer semiconducting layer;
- A comparison between the transmission characteristics of two power cables of varying length, 8.25 m and 20 m; and
- A comparison between a power cable and a typical communication cable (RG58) cable of the same length.

The quantification of the effect of the outer semiconducting layer is the main focus of this report, and was the main focus of the testing procedure as mentioned in the research question in *Section 2.6*. It was important, however, to gain knowledge on the effects of length and the type of cable to further understand the ability of MV power cables to transmit HF signals and the influence of the outer semiconducting layer. Comparative measurements of the cable with and without the outer semiconducting layer were performed on equal lengths of cable therefore eliminating variations that could be due to length.

The next section details an alternative testing methodology which uses a network analyser to obtain the HF response of a power cable.

## 4.2 The Network Analyser Method

As the power cable is a type of transmission medium, a possible means of obtaining the HF characteristics of a power cable is through the use of a network analyser [13]. A network analyser measures the network parameters of an electrical network [13]. In transmission line theory, the key component that needs to be determined is the scattering matrix or S-parameter matrix, which allows for the characterisation of the transmission line. A scattering matrix is used to show the relationship between variables  $a_n$  and  $b_n$  [18]. Figure 4.1 shows a 2-port network, with the variables being related by *Equation (4.1)*. To obtain measurements using the network analyser, one port or the other is terminated with a normalising impedance  $Z_0$ , which is usually  $50 \Omega$ .

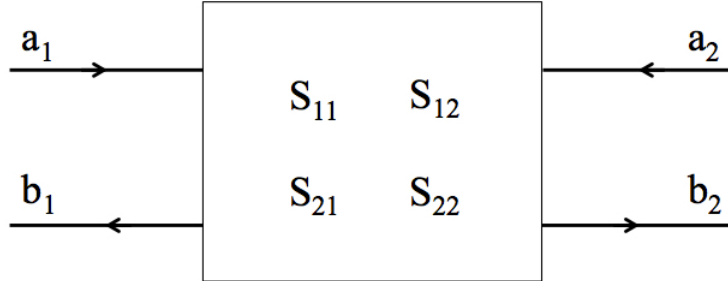


Figure 4.1: Two port S-parameter network

The reflection and transmission coefficients are then directly expressed in terms of the scattering parameters [13]. However, a calibration procedure is often necessary due to the fact that it is often not possible to directly connect the device under test without the use of adapters, which causes an impedance mismatch.

$$\begin{bmatrix} b_1 \\ b_2 \end{bmatrix} = \begin{bmatrix} S_{11} & S_{12} \\ S_{21} & S_{22} \end{bmatrix} \begin{bmatrix} a_1 \\ a_2 \end{bmatrix} \quad (4.1)$$

An alternative approach, that allows for easier analysis of cascaded network is the use of the T-parameters, which are related to the S-parameters [13]. The T-parameters are defined as:

$$\begin{bmatrix} b_1 \\ b_2 \end{bmatrix} = \begin{bmatrix} T_{11} & T_{12} \\ T_{21} & T_{22} \end{bmatrix} \begin{bmatrix} a_1 \\ a_2 \end{bmatrix} \quad (4.2)$$

The T-parameters are related to the S-parameters as follows [13]:

$$\begin{bmatrix} S_{11} & S_{12} \\ S_{21} & S_{22} \end{bmatrix} = \begin{bmatrix} \frac{T_{12}}{T_{22}} & T_{11} - \frac{T_{12}T_{21}}{T_{22}} \\ \frac{1}{T_{22}} & -\frac{T_{21}}{T_{22}} \end{bmatrix} \quad (4.3)$$

$$\begin{bmatrix} T_{11} & T_{12} \\ T_{21} & T_{22} \end{bmatrix} = \begin{bmatrix} S_{12} - \frac{S_{11}S_{22}}{S_{21}} & \frac{S_{11}}{S_{21}} \\ -\frac{S_{22}}{S_{21}} & \frac{1}{S_{21}} \end{bmatrix} \quad (4.4)$$

Further measurements are possible by using the network analyser including the input impedance and Voltage Standing Wave Ratio (VSWR).

The difficulty of the network analyser method is in the impedance matching of the device under test and the measurements system. Therefore, a TDR measurement methodology was chosen in the present work as impedance matching was not necessary. The TDR methodology is detailed in the next section.

### 4.3 The Chosen TDR Measurement Methodology

TDR is a commonly used method in determining the spatial location and nature of various objects. When used in power cables, it involves sending a pulse signal down the cable and making use of an oscilloscope to observe the reflected pulses. In power cables, TDR is mainly used for fault location as mentioned in *Section 2.2*.

In PD detection, if the length ( $L$ ) of the cable is known, it is possible to determine the location ( $x$ ) using the time difference between incident and reflected pulse as shown in *Equation (4.5)* [19].

$$x = L - \frac{1}{2}\Delta t.v \quad (4.5)$$

In the physical tests of the cable in this work, this technique will not be used for location determination but rather to determine how the reflections will differ with a change in the cables structure [13].

The TDR measurement procedure on the cable is as follows: first, a

typical standard power cable is tested under normal conditions. The signal generator is used to inject a high frequency signal into the cable. As shown in *Figure 4.2*, an oscilloscope is used to record the reflections. After the first test is completed, the cable is stripped of its outer semiconductor layer, and the cable reassembled. The same test is done on the cable and comparisons of measurement results made.

Each test case is performed multiple times to ensure that a significant amount of data is collected so that measurements considered outlying can be identified.

The TDR measurements were performed using the setup as shown in *Figure 4.2*. In the literature, a popular test signal is the impulse. An ideal impulse is infinitely high, with a zero width and an area of one, termed the Dirac delta function. However, this is theoretical and therefore cannot be reproduced in a laboratory [20]. Therefore the impulse used in this test would have a high rise time and a narrow width so as to obtain a higher frequency content within the test signal to be produced [20].

The impulse generator used produced a 5 V pulse with a 5 ns rise time, 20 ns width and a frequency of 300 kHz. The frequency of 300 kHz allows for a sufficient period in which the reflections would tend to zero before the next pulse is triggered. It must be noted that only the results from a single pulse and its subsequent reflections are analysed in this investigation.

It is also important to note that the ambient and core temperatures were to be kept constant for both tests (i.e. with and without the semiconductor layer) so that a comparison can be made between the results obtained. This was achieved by using temperature sensors at the cable core and the outer most layer of the cable. It is known that temperature affects the propagation of the HF signal [21] and therefore must be carefully noted and controlled in each test. In essence all the HF measurements should be done at the same temperature.

The incident and reflected pulses are recorded in the time domain using an oscilloscope, and by making use of Fourier Transforms, it is possible to analyse these in the frequency domain.

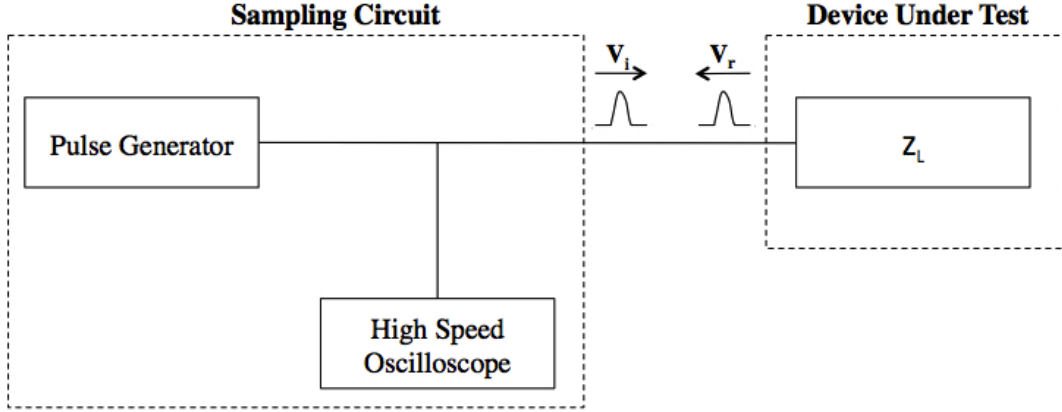


Figure 4.2: Time domain measurement setup

In the frequency domain, the propagation velocity, attenuation and phase constant are determined using the measured values. The transfer function,  $H(\omega)$  is calculated by taking the ratio of the Fast Fourier Transform (FFT) of the output (the reflected pulse  $V_{out}$ ) and the input (the incident pulse  $V_{in}$ , as given in *Equation* (4.6) [2, 22].

$$H(\omega) = \frac{FFT(V_{out})}{FFT(V_{in})} = e^{-Y(\omega)2L} \quad (4.6)$$

where:

$Y(\omega)$  is the propagation constant

$L$  is the cable length.

As the incident pulse travels the full length of the cable and then returns along the same length of the cable, after reflection on the open circuited cable end, a factor of 2 is introduced appropriately into *Equation* (4.6).

From *Equation* (4.6), the attenuation and phase constants are calculated using *Equations* (4.7) and (4.8) [22].



$$\alpha(\omega) = -\frac{1}{2L} \times \ln|H(\omega)| \quad (4.7)$$

$$\beta(\omega) = -\frac{1}{2L} \times \angle H(\omega) \quad (4.8)$$

## 4.4 Test Setup and Procedure

All experimentation was conducted in the Genmin Laboratory at the University of the Witwatersrand. The following equipment was used to obtain the results needed for this research project:

- Test cable;
- RIGOL DS6062 600 MHz Digital Oscilloscope;
- Hewlett Packard 8002A Pulse Generator;
- Mini Circuits Signal Splitter ZFRSC-2050; and
- 3 x 1 m communication (RG-58) cable segments to connect the equipment and cable together.

Refer to *Figures 4.3, 4.4, 4.5, 4.6 and 4.7* for images of the above-mentioned components used in testing.

The RIGOL, DS6062, 600 MHz oscilloscope was chosen as to avoid distortion of the signal by the oscilloscope itself. For each measurement in the time domain the oscilloscope captured 14002 points of data, with a time division of  $2.00 \times 10^{-10}$  s. This was the largest number of data points that was possible in order to capture only a single pulse and the reflections.

The test equipment was set up as shown in *Figure 4.8*. The signal splitter was used to connect the pulse generator with both the cable under test and the oscilloscope.

As the impulse generator produced an impulse train, the oscilloscope was setup to only capture the data for a single pulse.



Figure 4.3: 8.25 m 11 kV single core cable used in testing



Figure 4.4: RIGOL DS6062 600 MHz Digital Oscilloscope



Figure 4.5: Hewlett Packard 8002A Pulse Generator

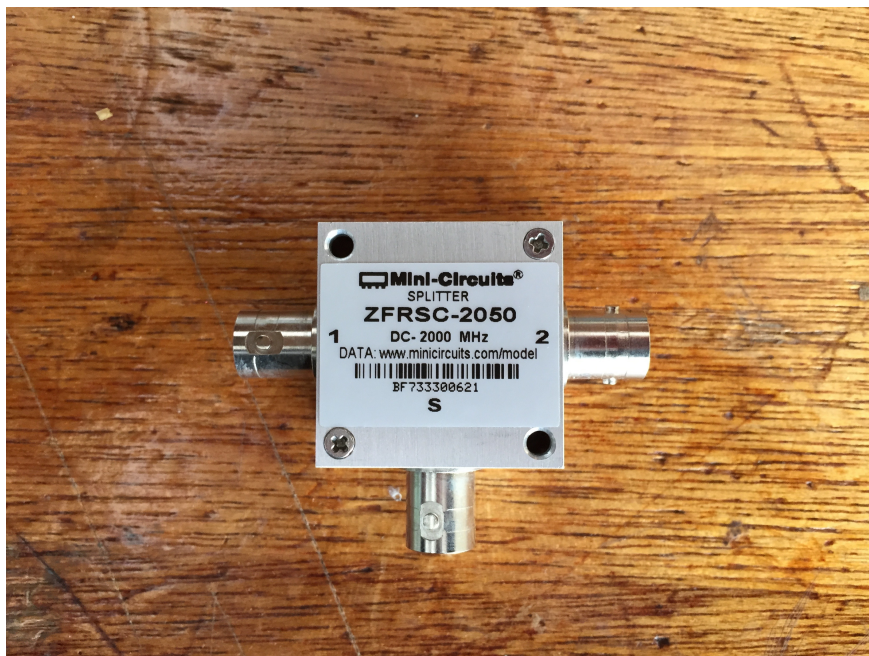


Figure 4.6: Mini Circuits Signal Splitter ZFRSC-2050



Figure 4.7: 1 m communication (RG-58) cable segments

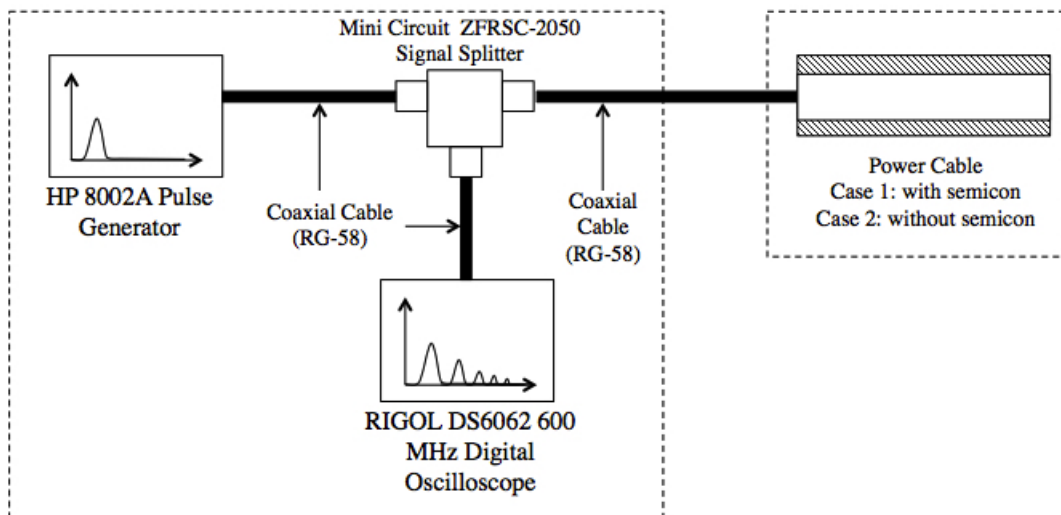


Figure 4.8: TDR experimental setup

Furthermore, the oscilloscope was set to capture the maximum number of points to provide a better accuracy.

An import factor to consider during the testing procedure is the temperature at which the testing is done. It has been determined in Nyamupangedengu, *et al*, (2015) [2] and Li, *et al*, (2005) [21] that the HF characteristics of a power cable will change with a change in temperature. Nyamupangedengu, *et al*, (2015) [2] had done work in determining the change in the HF characteristics for a 11 kV single power cable at temperature of 25° C, 45° C and 60° C. It was measured that the propagation velocity of a pulse travelling within an MV power cable will increase in the order of 4% as the temperature of the cable's core increase for room temperature to around 60. Furthermore, there were changes in attenuation and phase constant with a change in temperature. It is therefore important that the testing environment is kept at a constant temperature so that variation in the HF characteristics do not occur due to temperature fluctuation. The temperature during testing was kept at room temperature, a range of 22 - 26 ° C.

The TDR test procedure used to capture the incident and reflected pulses is as follows and is also given as a flowchart in *Figure 4.9*:

- Firstly only connect the oscilloscope and pulse generator through the 3-way connector but without the test power cable.
- Switch on both oscilloscope and pulse generator. Ensure the correct pulse waveform is being generated. Note that the pulse generator temperature increases with time causing slight variations in the generated pulse after a long time. Therefore it is necessary to turn off the generator as soon as possible after the data has been captured for the experiment.
- Record the incident pulse data.
- Connect the device under test to 3-way connector and record the reflected pulses.
- Turn off equipment. Disconnect all devices.

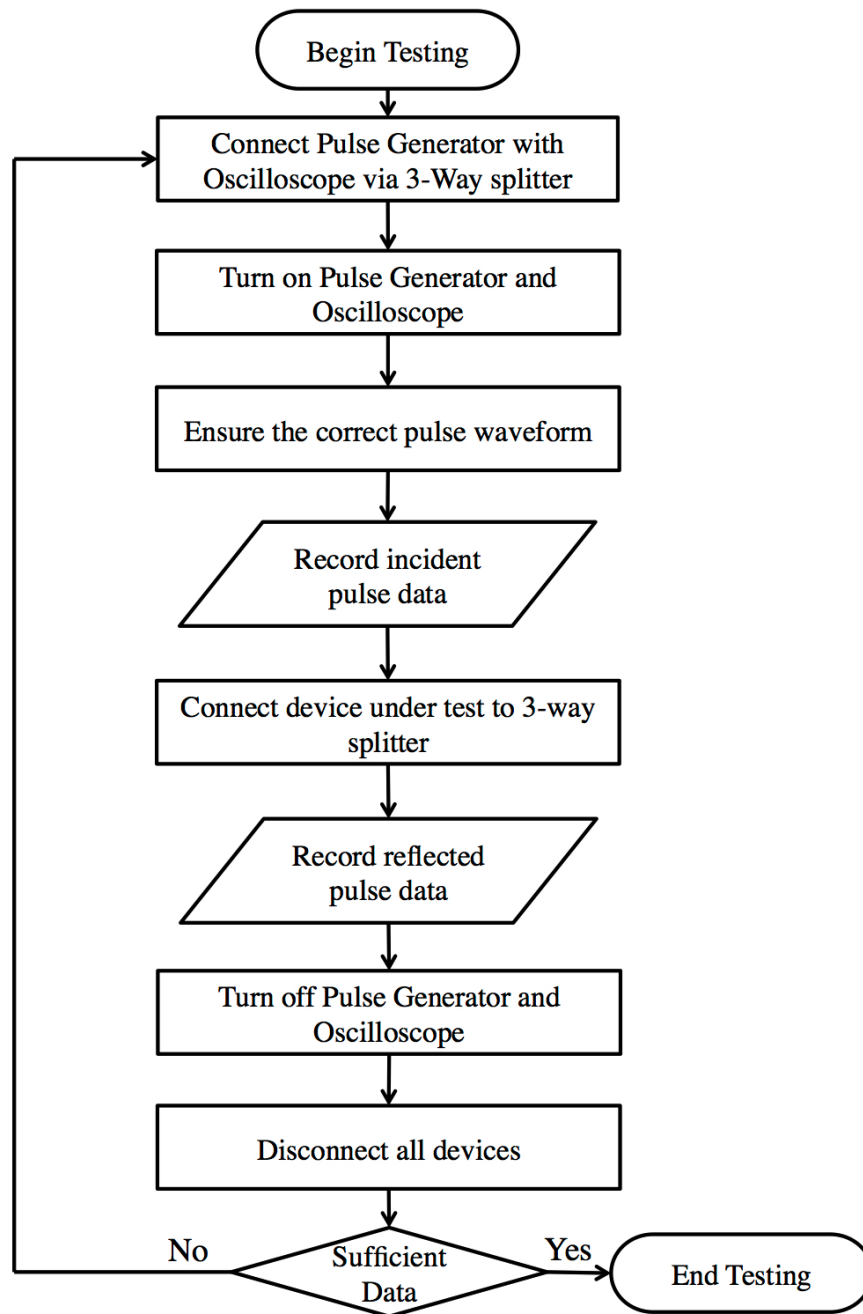


Figure 4.9: TDR test procedure flow chart

Each test was repeated multiple times. This was to ensure that a significant amount of data was collected in order to identify any outliers within the measurements and check on repeatability. The same test procedure was done for each of the test scenarios.

## 4.5 Different Test Cases

Quantification of the effect of the outer semiconducting layer on the HF characteristics was the focus of the testing procedure. Further testing was done to determine the effect of cable length on the HF characteristics and further, a comparison was made between a typical communication cable, RG-58 cable, and a power cable.

Each test made use of the TDR method described in *Section 4.3*. It was important to ensure the same incident pulse was used in each test thus ensuring accurate calculations and comparisons. It must be noted that the incident pulse captured from the pulse generator without the test object connected was not used in the calculation of the HF frequency characteristics and rather the incident pulse that is present in the multiple reflection reading was used.

Three different test scenarios were conducted as presented in the following sections.

### 4.5.1 Comparative test of MV power cable of the same length with and without the outer semiconducting layer

The choice of cable length for this test was restricted by the availability of 11 kV MV power cable at the University and the feasibility of compactly reassembling the cable after the outer semiconducting layer was removed. An 8.25 m 11 kV single core power cable with XLPE insulation and copper tape shielding was used.

In order to assess the influence of the outer semiconducting layer, the power cable with its normal structure was tested first using the TDR method.

In order to assess the behaviour without the outer semiconducting layer, the outer semiconducting layer was removed and the cable retested. This was done by first removing the copper tape shield of the cable and the waterproofing tape. The outer semiconducting layer was carefully stripped, ensuring that no damage was done to the XLPE insulation. Once the outer semiconducting layer was removed, the power cable was then carefully reassembled so as to ensure that the copper tape shield was tightly fitted onto the XLPE insulation, leaving no gaps. Insulation tape was wrapped over the cable to tightly secure the metallic sheath. Again using the TDR method, the cable was tested. The results are presented and discussed in the next chapter.

#### **4.5.2 Comparative tests of MV power cables of different length**

A comparison was needed to understand the relationship between length and the HF characteristics of a standard power cable. Two MV power cables with the same structure, both 11 kV single core XLPE with copper tape shielding, were used. The first cable had a length of 8.25 m and the other 20 m. The 20 m length was chosen as it was the maximum length of cable available at the University and, being over double the length of the shorter cable, it was deemed a sufficient length to make an effective comparison on the effects of length on the HF characteristics. The results are presented and discussed in the next chapter.

#### **4.5.3 Comparative test of MV power cable and a communication cable of the same length**

Comparative HF measurement tests were made between an 8.25 m 11 kV single core XLPE with copper tape shielding power cable and an 8.25 m RG58C/U communication cable. This test was done to compare the power cable's HF transmission capabilities with a cable specifically designed for HF signal transmission. The results are presented and discussed in the next chapter.



# Chapter 5

## EXPERIMENTATION RESULTS AND DISCUSSION

### 5.1 Introduction

This chapter presents the detailed analysis of the data acquired during the TDR measurement processes, aimed at quantifying the effects of the outer semiconducting layer on the transmission of HF signals in MV power cables.

### 5.2 Calibration of the TDR Method

In order to validate the accuracy of the TDR method, the known lengths of two cables are calculated using the TDR method and compared with the actual measured length.

From *Figure 5.1*,  $t_1$  is  $1.23 \times 10^{-7}$  s and  $t_2$  is  $3.70 \times 10^{-7}$  s. In the literature the velocity of a pulse in the cable is generally assumed to be about 45% of that of light, that is  $1.35 \times 10^8$  m/s. Using *Equations (5.1)* and *(5.2)*, the length of cable 1 and 2 are calculated to be 8.30 m and 24 m respectively. The actual lengths of the cables were 8.25 m and 20 m respectively and therefore the TDR signal was reasonably accurate. The difference between the calculated and actual lengths could be due to the use of the estimated propagation velocity in the calculations.

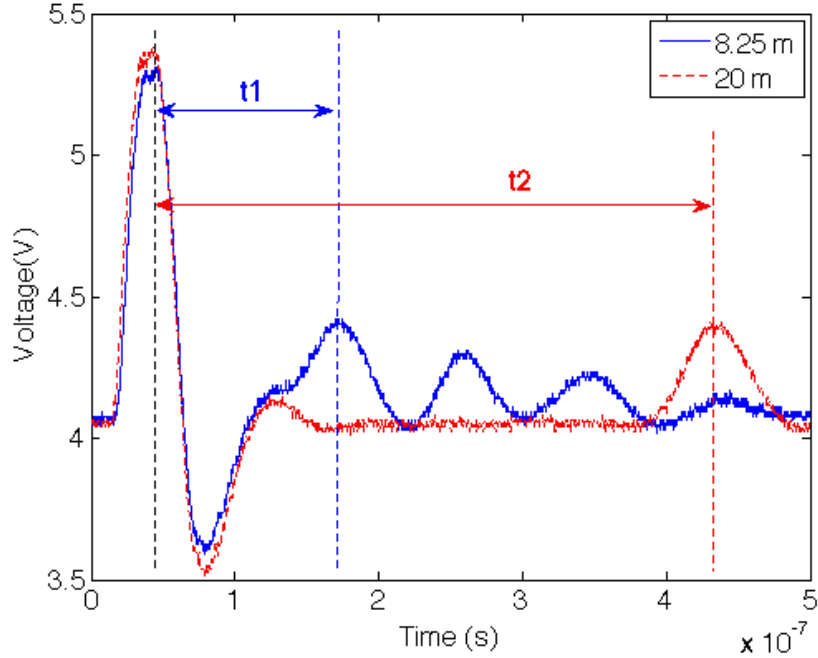


Figure 5.1: Time domain response of 8.25 m and 20 m power cable

Furthermore, as proven by Kreuger, *et al*, [3], errors in TDR techniques increase with length. In the present case, the error for the shorter cable (8.25 m) was 0.6% and the error for the longer cable (20 m) was 20%.

$$L_1 = \frac{V \times t_1}{2} \quad (5.1)$$

$$L_2 = \frac{V \times t_2}{2} \quad (5.2)$$

As a further calibration exercise, TDR measurement data of the same lengths of a power cable and a communication cable were plotted on the same axis as shown in *Figure 5.2*.

The time difference ( $t_1$ ) between the first and second pulse peaks of the RG 58 cable was calculated to be  $9.763 \times 10^{-8}$  s. The distance travelled by the pulse is 16.5 m. Therefore the velocity of the pulse is  $1.69 \times 10^8$  m/s.

Using *Equation (5.3)*, the velocity factor of the RG 58 was calculated to be 0.56. This is reasonably close to the expected value of 0.66 [23].

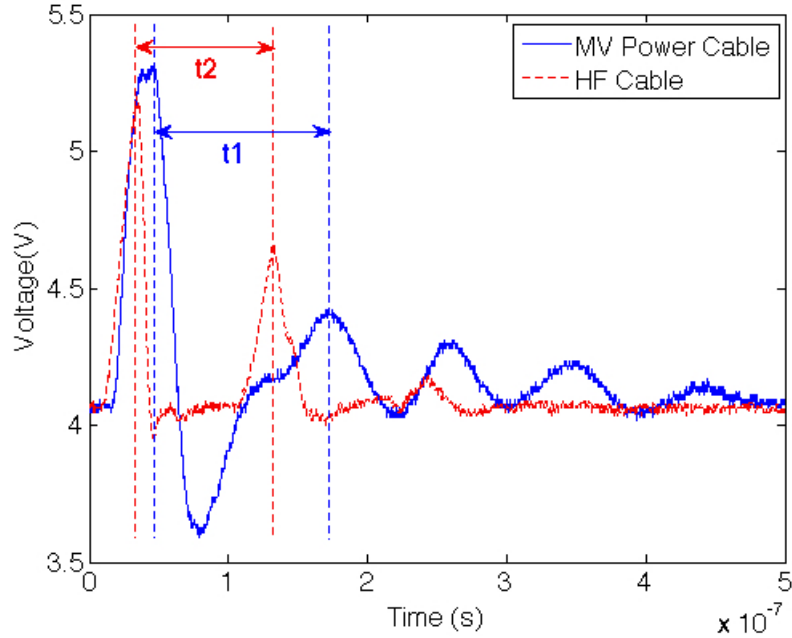


Figure 5.2: Time domain response of MV power cable and RG58 cable

In the comparison between the power cable and the RG-58, it is evident that the RG-58 cable is much more effective in transmitting HF signals as the velocity is far greater than that of the power cable, with the difference in velocity factor being 0.113 or 11.3%.

### 5.3 Time Domain Response

Plotted on the same axis, the multiple reflection traces of the pulses in the cable with (case 1) and without (case 2) the outer semiconducting layer is shown in *Figure 5.3*. It is evident that the plot of case 1 is shifted to the right relative to that of case 2. This implies that the pulse is faster in case 2 than in case 1. Similar findings were reported in Ametani, *et al*, (2004) [16].

The propagation velocity in communication channels is often expressed as the velocity factor as given in *Equation (5.3)*.

The velocity factor is important in some cable applications such as fault location and communication.

$$VF = \frac{v}{c} \quad (5.3)$$

Where:

$VF$  is the velocity factor; the ratio of the speed of the pulse in the cable ( $v$ ) to that of light ( $c$ ),  $3 \times 10^8$  m/s.

In order to calculate the velocity of the pulse in the cable, the time taken for the pulse to travel twice the length of the cable needed to be determined. This was done by determining the time difference between the first peak and the second peak, or any two consecutive peaks. Once the time and distance were known, the velocity could be determined. Then making use of *Equation (5.3)*, the velocity factor for the cable could be determined.

The pulse gets distorted as it travels along a power cable. This distortion can introduce errors when comparing two pulses. Using the time difference between two peaks of consecutive pulses gives a more accurate time of flight value when compared to alternatives such as the use of the zero crossing point [3].

The time difference between the first and second pulse peaks ( $t_1$ ), in *Figure 5.3*, for the power cable with the outer semiconducting layer, was calculated to be  $1.23 \times 10^{-7}$  s. The total return path distance travelled by the pulse is 16.5 m. Therefore the velocity of the pulse is  $1.34 \times 10^8$  m/s.

For the case of the cable without the outer semiconducting layer, the time difference between the first and second pulse peaks ( $t_2$ ), in *Figure 5.3*, was calculated to be  $1.17 \times 10^{-7}$  s. The distance travelled by the pulse is 16.5 m. Therefore the velocity of the pulse is  $1.41 \times 10^8$  m/s.

Using *Equation (5.3)*, the velocity factor for the power cable, with and without the semiconducting layer, was calculated. For the standard power cable, the velocity factor was calculated to be 0.447. This is similar to velocity factor values calculated in [3, 24] which confirms the efficacy of the measurement method. For the power cable without the outer semiconducting layer,

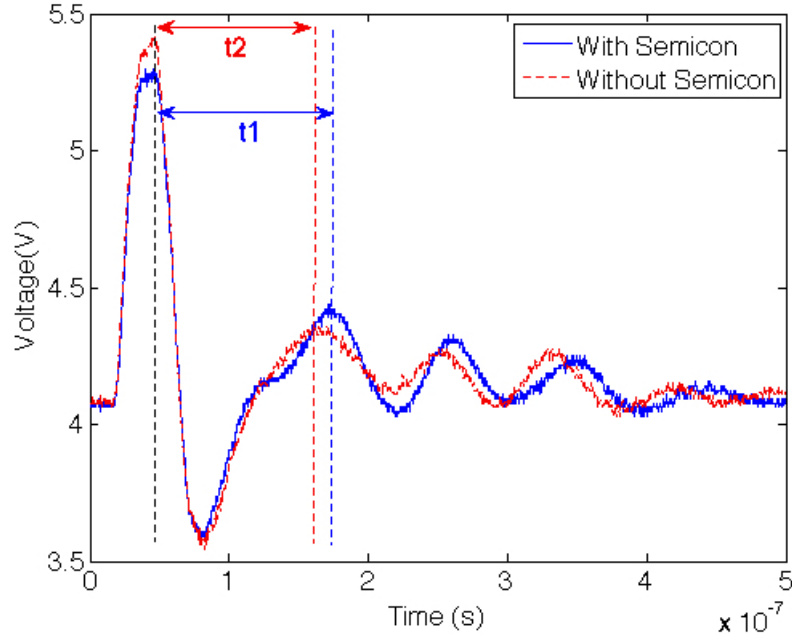


Figure 5.3: Time domain response of MV power cable with and without the outer semiconducting layer

the velocity factor is calculated to be 0.47. From a comparison between the two velocity factor values, it can be seen that the outer semiconducting layer has an effect on the propagation velocity of the pulse, increasing the velocity by 5.15%.

## 5.4 Frequency Domain Response

This section comprises of the analysis in the frequency domain. *Equations* (5.4) and (5.5) are computed in Matlab<sup>®</sup> using the code given in *Appendix A.2*.

Using the measured frequency components of the signal the attenuation and phase constant are calculated using *Equations* (5.4) and (5.5) respectively [2].

$$\alpha(\omega) = \text{Re} \left[ -\frac{1}{2L} \cdot \ln \left( \frac{\text{FFT}(V_{out})}{\text{FFT}(V_{in})} \right) \right] \quad (5.4)$$

$$\beta(\omega) = \text{Im} \left[ -\frac{1}{2L} \cdot \ln \left( \frac{FFT(V_{out})}{FFT(V_{in})} \right) \right] \quad (5.5)$$

For each case  $FFT(V_{in})$  is the Fourier Transform of the 1st pulse (incident) while  $FFT(V_{out})$  is that of the corresponding reflected pulse.

Plots of the  $v$ ,  $\alpha(\omega)$  and  $\beta(\omega)$  are produced for the power cable for the 2 cases of with and without the outer semiconducting layer. The plots are further compared with those produced through simulations using Mugala's model [13] as presented earlier in *Chapter 3* of this project.

The HF characteristics of the cable were analysed between the frequency range of 1 to 30 MHz, as it is stated in [3] that a cable has a usable bandwidth up to 10 to 20 MHz, which is based on past studies on the measured attenuation of high frequency signals in solid dielectric cables. Such range falls in the middle of the frequency range used in the frequency domain analysis. It is useful to assess how the measured HF response behaves on either side of the usable bandwidth.

It must be noted that the 8.25 m power cable was used as the reference for all comparative analysis within this section.

### 5.4.1 Attenuation

*Figure 5.4* is a plot of attenuation as a function of frequency for cases of a power cable with and without the outer semiconducting layer present.

The mean attenuation of the cable with the outer semiconducting layer is 0.472 dB/m and the cable without is 0.467 dB/m in the frequency range of 1 to 7 MHz. For the frequency range of 7 to 30 MHz, the mean attenuation of the cable with the outer semiconducting is 0.726 dB/m and the cable without is 1.010 dB/m. The mean attenuation difference between the power cable with and without the outer semiconducting layer from 1 to 7 MHz is about 1.14%. It is evident from these values that the outer semiconducting layer of the power cable does have an effect on the attenuation. However,

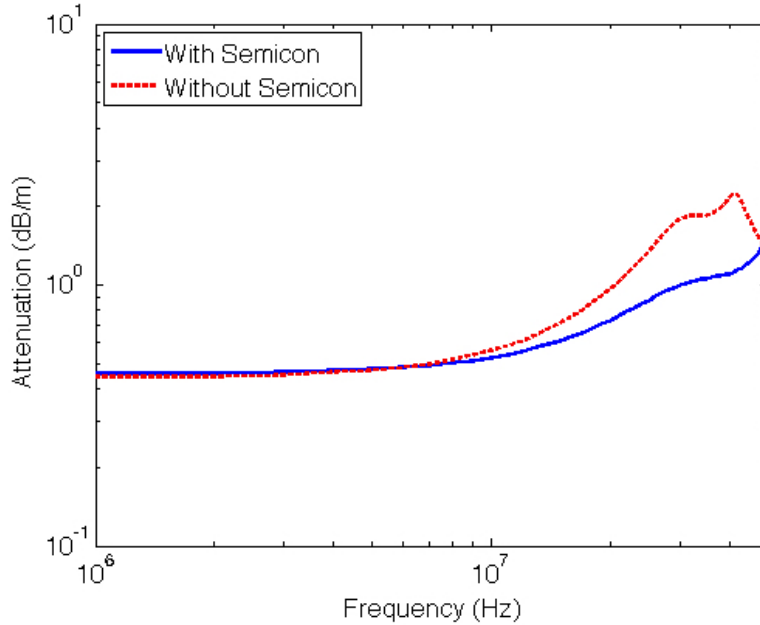


Figure 5.4: The change in attenuation of MV power cable with and without the outer semiconducting layer as a function of frequency

the variation in the attenuation from 1 to 7 MHz is relatively small when compared to the 3.08% obtained through simulations. For frequencies larger than 10 MHz the power cable is not suitable for HF transmission as the attenuation values for both cases significantly increase which correlates with the simulations and [16].

For both cases, the attenuation is a function of frequency. This is supported by the fact that the attenuation of the power cable with the outer semiconducting layer increases from 0.46 dB/m at 1 MHz to 0.52 dB/m at 10 MHz, which is an increase of 13%. From 10 to 20 MHz there is an increase of 0.22 dB/m (42.3%). For the attenuation of the power cable without the outer semiconducting layer, there is an increase from 0.44 dB/m at 1 MHz to 0.56 dB/m, which is an increase of 27%. From 10 to 20 MHz there is an increase of 0.43 dB/m (77%).

When a comparison is made between the physical measurement results and the estimated results obtained through the simulation of the theoretical HF model of the power cable, it is clear that the model accurately predicts

that the outer semiconductor layer has an effect on the HF characteristics of the power cable as the simulated results showed a mean difference of 3.08% for a range of 1 to 10 MHz and the experimental results gave a 1.14% difference for the range of 1 to 7 MHz. It is important to note that the model displays linear relationships between attenuation and phase constant with respect to frequency including large frequency values, which in reality it is not the case. Furthermore, for the attenuation values of the power cable, the simulation predicts significantly lower values for the range of 1 to 10 MHz.

When comparing the experimental attenuation values to literature, it is seen that the attenuation values from the experiment are generally larger although admittedly the attenuation parameter is naturally expected to vary across power cables of different construction, dimension and material composition.

The useful bandwidth of power cables is generally known to be approximately 20 MHz [3]. This concurs with experimentation results of the present work which shows that a much larger increase in attenuation occurs after the 20 MHz point. The attenuation values begin to oscillate after 20 MHz and can be considered noise.

In *Figure 5.5*, it is evident that the length of the cable has a significant affect on the attenuation of HF signals. It can clearly be seen that the usable bandwidth changes with length. With a shift in the usable bandwidth, it can be seen that there is a shift in the peak value of the attenuation from approximately 55 to 45 MHz. Between 1 to 20 MHz, the 8.25 m power cable has a mean attenuation of 0.558 dB/m and the 20 m power cable has a mean attenuation of 0.604 dB/m and represents a mean difference in attenuation of 8.25%. Beyond 20 MHz the signal is heavily distorted and resultant calculated attenuation values make little sense.

In *Figure 5.6*, it is evident that the RG-58 has a significantly less attenuation value for all frequencies compared to the same length of a power cable. The mean attenuation for the power cable between 1 to 30 MHz is 0.667 dB/m and for the RG-58 cable is 0.270 dB/m. This gives a mean difference about 60%.



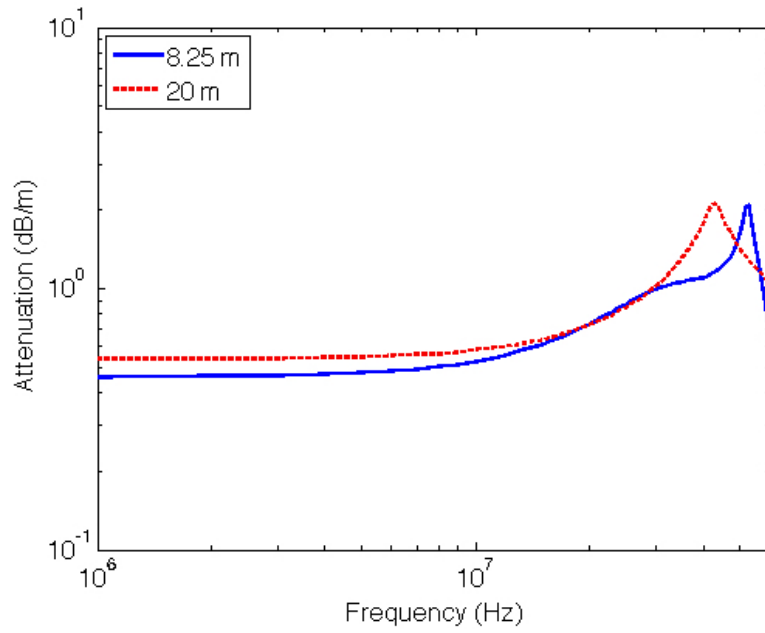


Figure 5.5: The change in attenuation of 8 m and 20 m MV power cable as a function of frequency

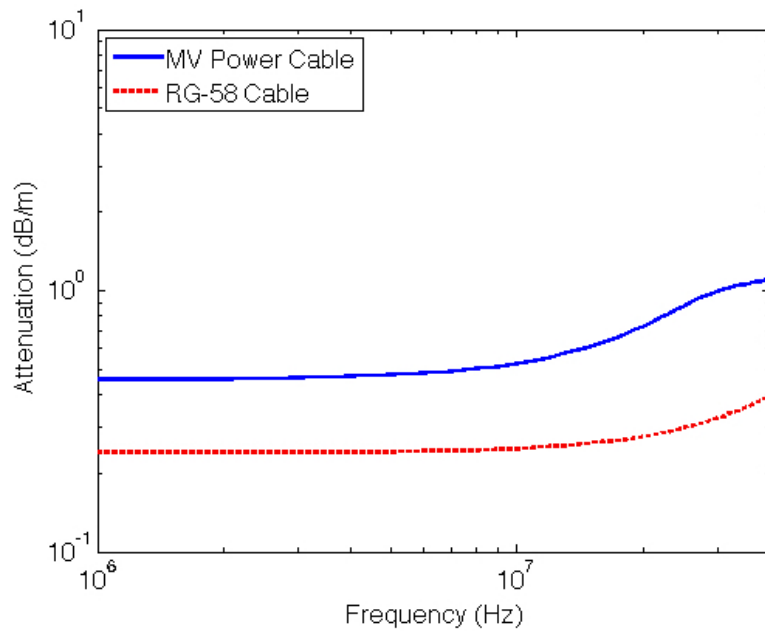


Figure 5.6: The change in attenuation of MV power cable and RG58 cable as a function of frequency

## 5.4.2 Phase Constant

The outer semiconducting layer has an effect on the phase constant of the cable, with an apparent difference between the two curves, as shown in *Figure 5.7*. The mean phase constant for the cable with the outer semiconducting layer is 0.064 rad/m and cable without is 0.044 rad/m for the frequency range of 1 to 20 MHz, and is a mean difference of 31.11% between the two curves. In comparing the results to those in the simulation, it can be seen in both *Figures 3.2* and *5.7* that the phase constant increases with an increase in the frequency. Furthermore, the increase is linear in both. However after 20 MHz the experimental results show a large deviation of the curve for the cable without the outer semiconducting layer. The results from the experiment show that there is a larger difference in the phase constant between the power cable with and without the outer semiconducting layer, (31.11%), when compared to the simulation, (3.82%).

In comparing the phase constant of the same length of power cable and communication cable as shown in *Figure 5.8*, it can be seen that there is a large difference between the two curves, with the power cable having a larger phase constant for the complete frequency range. The mean difference in the phase constant is about 90%.

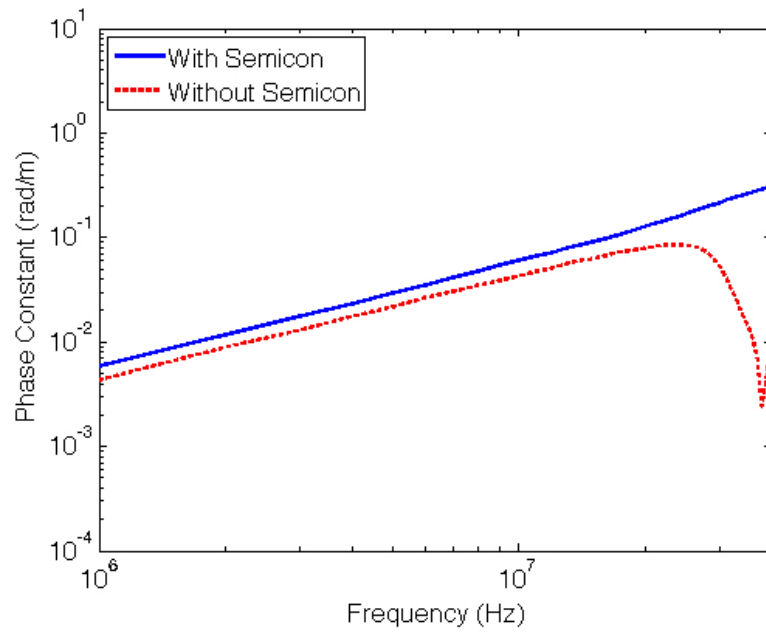


Figure 5.7: The change of the phase constant of MV power cable with and without the outer semiconducting layer as a function of frequency

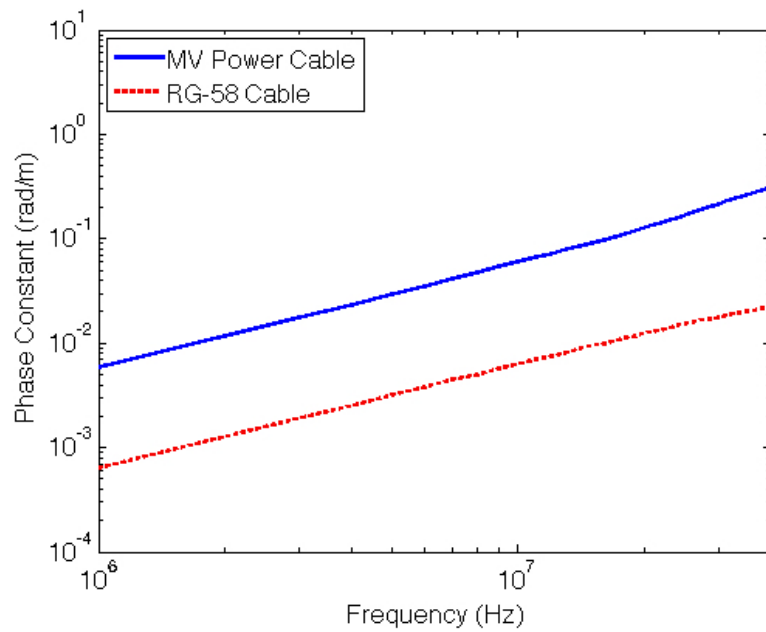


Figure 5.8: The change of the phase constant of MV power cable and RG58 cable as a function of frequency

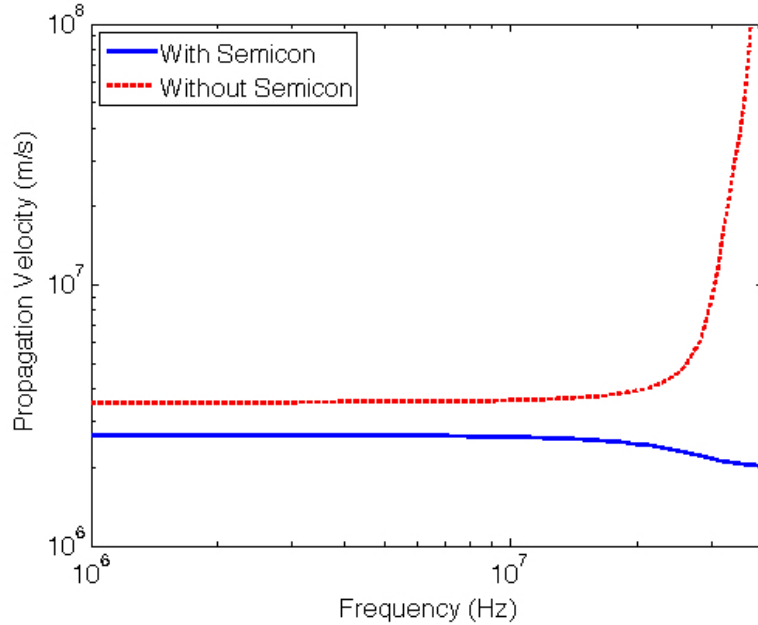


Figure 5.9: The change of the propagation velocity of MV power cable with and without the outer semiconducting layer as a function of frequency

### 5.4.3 Propagation Velocity

The outer semiconducting layer has an influence on the propagation velocity of HF signals within the power cable, as seen in *Figure 5.9*. The power cable with the outer semiconducting layer has a mean propagation velocity of  $2.560 \times 10^6$  m/s and the cable without the outer semiconducting layer has a mean value of  $3.666 \times 10^6$  m/s for the frequency range of 1 to 20 MHz. This results in a mean difference of 41.18% and further confirms the time domain results presented in *Section 5.3*, that the cable without the outer semiconducting layer has a larger propagation velocity. However, there is a large difference between the propagation velocity value determined in *Section 5.3* and that in *Figure 5.9*. The time domain based velocity difference calculation could be deemed less accurate due to the pulse distortions as explained earlier.

It is evident, in *Figure 5.10*, that the RG 58 cable has a significantly higher propagation velocity when compared to the power cable. The mean

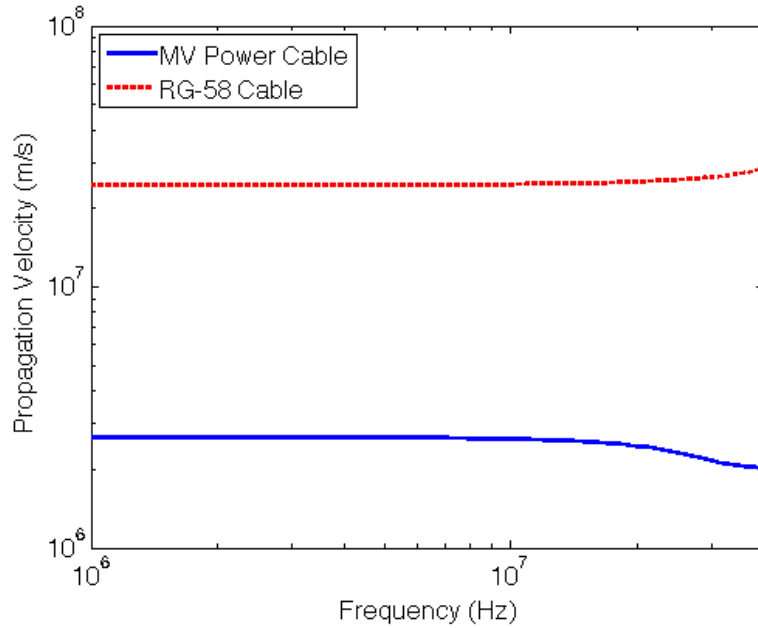


Figure 5.10: The change of the propagation velocity of MV power cable and RG58 cable as a function of frequency

propagation velocity of the power cable is  $2.560 \times 10^6$  m/s and the RG-58 cable value is  $2.488 \times 10^7$ , giving a mean difference between the two of 876%. This finding is consistent with the time domain findings in *Section 5.3*, where the RG-58 has a much greater velocity factor.

## 5.5 Summary of Results

From *Table 5.1*, it can be seen that there is a relatively small variations in the percentage difference of the attenuation values between the simulation and physical testing results. However, large and more significant differences are present between the phase constant and propagation velocity values.

The differences between the simulation and physical testing results can be reduced by, firstly, obtaining the exact complex permittivity values for the various layer of the physical cable rather than using approximate values. Secondly, the exact conductor screen values used may vary from the values used in the simulation source code, as seen in *Appendix A.1*. Finally, the

intervals between the data points can be reduced and the number of data points increased in the simulations. In fine tuning these variables it may be possible to reduce the differences in the these values.

Table 5.1: Comparison of Simulated and Physical Results

	Percentage Difference of Attenuation (%)	Percentage Difference of Phase Constant (%)	Percentage Difference of Propagation Velocity (%)
Simulation	3.08	3.82	4.2
Physical	1.14	31.11	41.18

Table 5.2: Comparison between Power Cable With and Without Outer Semi-conducting Layer

	Mean Difference Attenuation (dB/m)	Mean Difference Phase Constant (rad/m)	Mean Difference Propagation Velocity (m/s)
Frequency (MHz)	1 - 7	1 - 20	1 - 20
With Semicon	0.472	0.064	$2.560 \times 10^6$
Without Semicon	0.467	0.044	$3.666 \times 10^6$
Percentage Diff	1.14%	31.11%	41.18%

Table 5.3: Comparison between Power Cable and RG-58 Cable

	Mean Difference Attenuation (dB/m)	Mean Difference Phase Constant (rad/m)	Mean Difference Propagation Velocity (m/s)
Frequency (MHz)	1 - 30	1 - 30	1 - 30
Power Cable	0.667	0.101	$2.560 \times 10^6$
RG-58	0.270	0.0096	$2.488 \times 10^7$
Percentage Diff.	60%	90%	876%

## 5.6 Conclusion

Using TDR measurement techniques, and results analysis in both time domain and frequency domain, the findings can be summarised as follows:

The velocity factor of the power cable is affected by the outer semiconducting layer with an increase of 5.15% for the power cable without the outer semiconducting layer.

The attenuation of the power cable is proportional to the frequency as there is an increase in attenuation with an increase in frequency. The attenuation of the power cable with the outer semiconducting layer increases by 13% from 1 MHz to 10 MHz and by 42.3% from 10 to 20 MHz. This is also evident in the simulations with an increase of 1567% in attenuation from 1 to 100 MHz.

The outer semiconducting layer increases the measured attenuation of the power cable by 1.14%. This is relatively small when compared to the 3.08% obtained through simulations.

Unlike the relatively small influence on the attenuation of the power cable, the outer semiconducting layer has greater effect on both the phase constant and propagation velocity with differences of 31.1% and 41.18% respectively. These difference are significantly larger than those obtained through simulations.

Through experimentation, it was observed that the useful bandwidth of the power cable is up to 20 MHz. Beyond 20 MHz the signal is heavily

distorted and resultant calculated attenuation values make little sense.

The length has an effect on the attenuation of the cable with an increase of 8.25% from the attenuation of the 8.25 m to 20 m cable. Further the length affects the usable bandwidth of the cable with a shift of the peak attenuation from 55 to 45 MHz.

In comparing the HF parameters of the different cable types of the same length, it was seen that the communication (RG-58) cable is much better suited for HF transmission than the power cable. The communication cable has a lower mean attenuation of about 60%, a smaller phase constant of about 90% and faster propagation velocity of 876% for the frequency range of 1 to 20 MHz.



# Chapter 6

## CONCLUSION

There is need to understand the contribution of each component of the structure of a power cable to the HF communication characteristics of the cable. The focus of this research report was to assess the influence of the outer semiconducting layer on the HF transmission characteristics of MV power cables.

The experimental investigation was done in two steps. Firstly, the influence of the outer semiconducting layer using established HF power cable models was simulated. Secondly, physical testing was performed on various cases using a TDR based measurement system.

Analysis of the simulated and experimental results was carried out to determine the effects of the outer semiconducting layer on the HF transmission parameters of the cable namely; velocity factor, attenuation, phase constant and propagation velocity. The summary of the findings of this research report are as follows;

The attenuation of a power cable is proportional to the frequency, as there is an increase in attenuation with an increase in the frequency.

The outer semiconducting layer of a power cable has an effect on the attenuation of the power cable with difference of 1.14% in the physical experimentation results, which is relatively small when compared to the 3.08% in the simulated results. The outer semiconducting layer however does have a larger effect on both the phase constant and propagation velocity with

differences of 31.1% and 41.18% respectively.

In comparing the simulated and physical test results, it was seen that the trend of the HF parameters with respect to frequency are the same. The difference however between the two sets of results is evident in the magnitude of the values and the mean differences between them.

The length of the power cable has an effect on the attenuation of the cable with an increase of 8.25% in the attenuation of the 8.25 m to 20 m cable. Furthermore the length affects the usable bandwidth of the cable with a shift of the peak attenuation from 55 to 45 MHz.

The comparison of the HF parameters of the power cable and communication (RG-58) cable confirms that power cables are not efficient transmitters of communication signals compared to communication cables that are specifically designed for communication.

This research report has shown that the outer semiconducting layer affects the HF transmission parameters of MV power cables and shows that there are limitations to using MV power cables for HF signal transmission. It is therefore imperative that the process of designing smart grid communication channels through power cables should take into account limitations due to the semiconducting layer among other components. Furthermore power cable designers should begin applying their efforts towards restructuring the power cable to be able to operate effectively as conveyers of both electric power and communication signals.

Future work would include testing on the relationship between the effect of the outer semiconducting layer with the temperature of the power cable. During the testing phase of this research report, ambient temperature was used. It is noted that during operation, a power cable will experience large fluctuations in temperature, i.e. moving from no-load to full load. Literature has suggested that there are variations in the HF parameters of power cables with respect to temperature. It would be of importance therefore to determine the correlation between the effect of the outer semiconducting layer and changes in temperature.

# REFERENCES

- [1] J. Liu, B. Zhao, J. Wang, Y. Zhu, and J. Hu. “Application of power line communication in smart power Consumption.” In *2010 IEEE International Symposium on Power Line Communications and Its Applications (ISPLC)*, pp. 303–307. March 2010.
- [2] C. Nyamupangedengu, M. Sotsaka, G. Mhlangeni, L. Ndlovu, and S. Munilal. “Effect of Temperature Variations on Wave Propagation Characteristics in Power Cables.” *Research Journal of the South African Institute of Electrical Engineers, SAIEE*, vol. 106, no. 1, pp. 28–37, March 2015.
- [3] F. Kreuger, M. Wezelenburg, A. Wiemer, and W. Sonneveld. “Partial discharge. XVIII. Errors in the location of partial discharges in high voltage solid dielectric cables.” *IEEE Electrical Insulation Magazine*, vol. 9, no. 6, pp. 15–22, Nov 1993.
- [4] Z. Du, P. Willett, and M. Mashikian. “Performance limits of PD location based on time-domain reflectometry.” *IEEE Transactions on Dielectrics and Electrical Insulation*, vol. 4, no. 2, pp. 182–188, Apr 1997.
- [5] J. Steiner, P. Reynolds, and W. Weeks. “Estimating the location of partial discharges in cables.” *IEEE Transactions on Electrical Insulation*, vol. 27, no. 1, pp. 44–59, Feb 1992.
- [6] A. Cataliotti, V. Cosentino, D. Di Cara, P. Russotto, and G. Tine. “On the use of narrow band power line as communication technology for

- medium and low voltage smart grids.” In *2012 IEEE International Instrumentation and Measurement Technology Conference (I2MTC)*, pp. 619–623. May 2012.
- [7] V. Gungor, D. Sahin, T. Kocak, S. Ergut, C. Buccella, C. Cecati, and G. Hancke. “Smart Grid Technologies: Communication Technologies and Standards.” *IEEE Transactions on Industrial Informatics*, vol. 7, no. 4, pp. 529–539, Nov 2011.
- [8] A. Cataliotti, A. Daidone, and G. Tine. “A Medium-Voltage Cables Model for Power-Line Communication.” *IEEE Transactions on Power Delivery*, vol. 24, no. 1, pp. 129–135, Jan 2009.
- [9] H. Meng, S. Chen, Y. Guan, C. Law, P. So, E. Gunawan, and T. Lie. “A transmission line model for high-frequency power line communication channel.” In *International Conference on Power System Technology, 2002. Proceedings. PowerCon 2002*, vol. 2, pp. 1290–1295 vol.2. 2002.
- [10] A. Kosonen and J. Ahola. “Comparison of signal coupling methods for power line communication between a motor and an inverter.” *Electric Power Applications, IET*, vol. 4, no. 6, pp. 431–440, July 2010.
- [11] A. Tonello. “Advances in Power Line Communications and Application to the Smart Grid.” In *Tutorial at EUSIPCO 2012*, pp. 21–22. Aug 2012.
- [12] N. Pavlidou, A. Vinck, J. Yazdani, and B. Honary. “Power line communications: state of the art and future trends.” *IEEE Communications Magazine*, vol. 41, no. 4, pp. 34–40, April 2003.
- [13] G. Mugala. *High Frequency Characteristics of Medium Voltage XLPE Power Cables*. Ph.D. thesis, The Royal Institute of Technology (KTH), Stockholm, Sweden, 2005.
- [14] G. Mugala, R. Eriksson, and P. Pettersson. “Dependence of XLPE insulated power cable wave propagation characteristics on design pa-

- rameters.” *IEEE Transactions on Dielectrics and Electrical Insulation*, vol. 14, no. 2, pp. 393–399, April 2007.
- [15] M. Tozzi, A. Cavallini, G. Montanari, and G. Burbui. “PD detection in extruded power cables: an approximate propagation model.” *IEEE Transactions on Dielectrics and Electrical Insulation*, vol. 15, no. 3, pp. 832–840, June 2008.
- [16] A. Ametani, Y. Miyamoto, and N. Nagaoka. “Semiconducting Layer impedance and its effect on cable wave-propagation and transient Characteristics.” *IEEE Transactions on Power Delivery*, vol. 19, no. 4, pp. 1523–1531, Oct 2004.
- [17] V. Dubickas and H. Edin. “On-line time domain reflectometry measurements of temperature variations of an XLPE power cable.” In *2006 IEEE Conference on Electrical Insulation and Dielectric Phenomena*, pp. 47–50. Oct 2006.
- [18] K. C. Gupta, R. Garg, and R. Chadha. *Computer Aided Design of Microwave Circuits*, pp. 25–43. Dedham, Massachusetts: Artech House Inc, 1981.
- [19] H. Borsi. “Digital location of partial discharges in HV cables.” *IEEE Transactions on Electrical Insulation*, vol. 27, no. 1, pp. 28–36, Feb 1992.
- [20] J. Andrew. *Time Domain Reflectometry (TDR) and Time Domain Transmission (TDT) Measurement Fundamentals*. Picosecond Pulse Labs, application note an-15 ed., Nov 2004.
- [21] Y. Li, P. Wouters, P. Wagenaars, P. van der Wielen, and E. Steennis. “Temperature Dependency of Wave Propagation Velocity in MV Power Cable.” In *The 18th International Symposium on High Voltage Engineering, 2013. ISH 2013*, pp. 1861–1866. Aug 2013.
- [22] G. Hashmi, R. Papazyan, and M. Lehtonen. “Determining wave propagation characteristics of MV XLPE power cable using time domain reflectometry technique.” In *International Conference on Electrical*

*and Electronics Engineering, 2009. ELECO 2009*, pp. I–159–I–163. Nov 2009.

- [23] Belden. *RG-58/U 9201 Detailed Specifications and Technical Data*. Belden Inc, 2012.
- [24] H. Blackburn, B. Phung, M. Vakilian, M. Naderi, and H. Zhang. “Investigation of high frequency signal propagation characteristics on HV XLPE cables.” In *The 7th International Power Engineering Conference, 2005. IPEC 2005*, pp. 776–781 Vol. 2. Nov 2005.

# Appendix A

## Matlab<sup>®</sup> Code

This appendix provides the source code used in the simulations in *Chapter 3*, and it further provides the source used in the analysis of the data captured in various physical testing scenarios detailed in *Section 4.5*.

### A.1 Simulation

The code for the simulation was the implementation of the equations presented in *Section 2.5*. The different sections in the code will be described using the Matlab comment delimiter, %.

#### SimulationModel.m

```
1 %Simulation of High Frequency Signal Transmission (Power ...
   Cable)
2
3 clc
4 clear all
5
6 %Copper Tape Metallic Screen
7
8 %%%%%%%%%%%%%%%%%%%%%%%%%%%%%%%%%%%%%%%%%%%%%%%%%%%%%%%%%%%%%%%%%%%%%%%%%
9
10 %Cable Parameters
11
```

```

12 e0 = 8.841941283e-12
13
14 %Conductor Screen Parameters
15
16 al_con = 0.35; %broadnes of relaxation
17 T1_con = 1100; %relaxation times
18 A1_con = 910; %amplitude factors
19 a2_con = 0.42; %broadnes of relaxation
20 T2_con = 10; %relaxation times
21 A2_con = 210; %amplitude factors
22 inf_con = 4; %high frequency component of the relative ...
    permeability
23 DC_con = 25; %dc conductivity
24
25 %Physcial Dimension of Cable Structure for Standard Cable
26 r1 = 6.75; %Conductor
27 r2 = 7.75; %Inner Semiconducting Layer
28 r3 = 11; %XLPE insulation
29 r4 = 11.7; %Outer Semiconducting Layer
30 r5 = 13.7; %Screen Bed
31
32 %Physcial Dimension ofCable Structure for Cable without ...
    Outer Semicon
33 R1 = 6.75; %Conductor
34 R2 = 7.75; %Inner Semiconducting Layer
35 R3 = 11; %XLPE Insulation
36 R4 = 13; %Screen Bed
37
38 u0 = 1.256637061e-6;
39 T0 = 20;
40 n = 44;
41
42 %Read in Freqency Values
43 f = xlsread('PermittivityMugala.xlsx','A4:A12');
44 w = 2*pi*f;
45
46 %Conductor Screen Values
47 e1_con = 1 - al_con;
48 p1_con = (w*T1_con*i).^e1_con;

```



```

49 e2_con = 1-a2_con;
50 p2_con = (i*w*T2_con).^e2_con;
51
52 term1_con = A1_con ./ (1 + p1_con);
53 term2_con = A2_con ./ (1 + p2_con);
54 term3_con = DC_con ./ (i*w*e0);
55
56 %Screen Bed Values
57 scbR25 = xlsread('PermittivityMugala.xlsx','C17:C25'); %Real
58 scbI25 = xlsread('PermittivityMugala.xlsx','J17:J25'); %Imag
59
60 %Insulation Screen
61 insR25 = xlsread('PermittivityMugala.xlsx','C4:C12'); %Real
62 insI25 = xlsread('PermittivityMugala.xlsx','J4:J12'); %Imag
63
64 %Permittivity
65 e_xlpe = 2.3 - i*0.001;
66 e_ins25 = insR25 - i*insI25;
67 e_scb25 = scbR25 - i*scbI25;
68 e_con25 = e_scb25;
69
70 T25 = 25; %Temperature
71
72 p6_25 = 1.68e-8*(1 + 0.003862*(T25-T0));
73 p1_25 = p6_25;
74
75 %%%%%%%%%%%%%%%%%%%%%%%%%%%%%%%%%%%%%%%%%%%%%%%%%%%%%%%%%%%%%%%%%%%%%%%%%
76 %Calculations for Standard Cable
77
78 %Admittance Values for Each Layer
79 y21 = (i.*w*2*pi*e0.*e_con25)./log(r2/r1);
80 y31 = (i.*w*2*pi*e0.*e_xlpe)./log(r3/r2);
81 y41 = (i.*w*2*pi*e0.*e_ins25)./log(r4/r3);
82 y51 = (i.*w*2*pi*e0.*e_scb25)./log(r5/r4);
83
84 %Cable Impedance Calculation (Copper Tape)
85 Z_1 = ((1/(2*pi*r1))*sqrt(i*w*u0*p1_25)) + ...
      (i*f*u0*log(r5/r1)) + (1/(2*pi*r5))*sqrt(i*w*u0*p6_25);
86

```

```

87 %Total Admittance of Cable
88 Y1 = 1 ./ ((1./y21) + (1./y31) + (1./y41) + (1./y51));
89
90 %Propagation Constant
91 Prop_const_1 = sqrt(Z_1.*Y1);
92
93 %Attenuation Constant
94 atten1 = real(Prop_const_1)*(20/log(10));
95
96 %Phase Constant
97 phase1 = imag(Prop_const_1);
98
99 %Propagation Velocity
100 velocity1 = w./imag(Prop_const_1);
101
102 %%%%%%%%%%%%%%%%%%%%%%%%%%%%%%%%%%%%%%%%%%%%%%%%%%%%%%%%%%%%%%%%%%%%%%%%%
103 %Calculations for Cable Without Outer Semicon
104
105 %Admittance Values for Each Layer
106 y22 = (i.*w*2*pi*e0.*e_con25)./log(R2/R1);
107 y32 = (i.*w*2*pi*e0.*e_xlpe)./log(R3/R2);
108 y42 = (i.*w*2*pi*e0.*e_scb25)./log(R4/R3);
109
110 %Cable Impedance Calculation for Cable Without Outer ...
    Semicon (Copper Tape)
111 Z_2 = ((1/(2*pi*R1))*sqrt(i*w*u0*p1_25)) + ...
    (i*f*u0*log(R4/R1)) + (1/(2*pi*R4))*sqrt(i*w*u0*p6_25);
112
113 %Total Admittance of Cable Without Outer Semicon
114 Y2 = 1 ./ ((1./y22) + (1./y32) + (1./y42));
115
116 %Propagation Constant
117 Prop_const_2 = sqrt(Z_2.*Y2);
118
119 %Attenuation Constant
120 atten2 = real(Prop_const_2)*(20/log(10));
121
122 %Phase Constant
123 phase2 = imag(Prop_const_2);

```

```

124
125 %Propagation Velocity
126 velocity2 = w./imag(Prop_const_2);
127
128 %%%%%%%%%%%%%%%%%%%%%%%%%%%%%%%%%%%%%%%%%%%%%%%%%%%%%%%%%%%%%%%%%%%%%%%%%
129 %Calculations
130
131 %Calculating mean and mean difference of the attenuation
132 diffAtten_1 = atten1(4:6)-atten2(4:6);
133 AttenMean_1 = mean(diffAtten_1);
134 MeanSemi_1 = mean(abs(atten1(4:6)));
135 MeanSemi_2 = mean(abs(atten2(4:6)));
136 perc_1 = AttenMean_1/MeanSemi_1*100;
137
138 %Calculating mean difference of phase constant
139 diffPhase_1 = phase1(4:8)-phase2(4:8);
140 PhaseMean_1 = mean(diffPhase_1);
141 MeanPhase_1 = mean(abs(phase1(4:8)));
142 MeanPhase_2 = mean(abs(phase2(4:8)));
143 perc_2 = PhaseMean_1/MeanPhase_2*100;
144
145 %Calculating mean difference of phase constant
146 diffVel_1 = velocity2(4:8)-velocity1(4:8);
147 VelMean_1 = mean(diffVel_1);
148 MeanVel_1 = mean(abs(velocity1(4:8)));
149 MeanVel_2 = mean(abs(velocity2(4:8)));
150 perc_3 = VelMean_1/MeanVel_1*100;
151
152 %%%%%%%%%%%%%%%%%%%%%%%%%%%%%%%%%%%%%%%%%%%%%%%%%%%%%%%%%%%%%%%%%%%%%%%%%
153 %Graph Plotting
154
155 %Attenuation Plot
156
157 fig = figure(1);
158 set(gca, 'FontSize',16, 'fontWeight', 'bold');
159 set(gcf, 'color', [1 1 1]);
160 loglog(f, atten1, '-ob', f, atten2, ':*r', 'LineWidth',1.25);
161 axis([10E5 10E7 10E-5 10E0]);
162 ylabel('Attenuation (dB/m)');

```

```

163 xlabel('Frequency (Hz)');
164 h1 = legend('With Semicon','Without Semicon');
165 set(h1, 'Location','Northwest');
166
167 %Phase Constant Plot
168 figure(2)
169 set(gca,'FontSize',16,'fontWeight','bold');
170 set(gcf,'color',[1 1 1]);
171 loglog(f, phase1,'-ob',f,phase2,':*r','LineWidth',1.25)
172 axis([10E5 10E7 10E-3 10E0]);
173 ylabel('Phase Constant (rad/m)')
174 xlabel('Frequency (Hz)')
175 h2 = legend('With Semicon','Without Semicon')
176 set(h2, 'Location','Northwest')
177
178 %Propagation Velocity Plot
179 figure(3)
180 set(gca,'FontSize',16,'fontWeight','bold')
181 loglog(f,velocity1,'-ob',f,velocity2,':*r','LineWidth',1.25)
182 set(gcf,'color',[1 1 1]);
183 axis([10E5 10E7 138038426 147910838]);
184 ylabel('Propagation velocity (m/s)')
185 xlabel('Frequency (Hz)')
186 h3 = legend('With Semicon','Without Semicon')
187 set(h3, 'Location','Northwest')

```

## A.2 TDR Analysis

The code for the TDR was the implementation of the equations presented in *Section 4.3*.

### A.2.1 Function Files

The TDR analysis was the same for each test, therefore functions were created so as to reduce redundant code.

#### FreqDomain.m

```
1 function [atten1, phase1, velocity1] = FreqDomain(incid1, ...
    reflect1, w, length)
2
3 %Frequency Caluclations
4
5 H_norm1 = fft(reflect1)./fft(incid1);
6 [Fp1, Fm1] = cart2pol(real(H_norm1), imag(H_norm1));
7 atten1 = (20/log(10))*(-1/(2*length)).*log(Fm1); %20/log20 ...
    is used to convert to dB/m
8 phase1 = (-1/(2*length)).*(unwrap(Fp1));
9 velocity1 = (2.5/1000)*w(1:512)./phase1(1:512);
10 p1 = (atten1 + i.*phase1);
11
12 end
```

The FreqDomain.m code is used to convert the time domain measurements into the HF characteristics. This is done by implementing the equations detailed in *Section 4.3*. The input of the function is the incident and reflected time domain waveforms and the outputs are the attenuation, phase constant and propagation velocity.

#### PlotTimeGraph.m

```
1 function PlotTimeGraph(reflect1, reflect2, timelength, ...
    increment, label1, label2)
2
```

```

3 %Plot Time Domain Response
4 figure(1)
5 set(gca,'FontSize',16,'fontWeight','bold');
6 set(gcf,'color',[1 1 1]);
7 plot(increment*timelength(1:2500), reflect1(1:2500), ...
      '-b',increment*timelength(1:2500), reflect2(1:2500), ...
      '--r')
8 xlabel('Time (s)')
9 ylabel('Voltage(V)')
10 h2 = legend (label1,label2);
11 set(h2, 'Location','NorthEast')
12 axis([0 0.5*10(-6) 3.5 5.5]);
13
14 end

```

The PlotTimeGraph.m code displays two reflected pulses. The inputs for the function are the reflected pulse vectors, the length of the vectors, the time increment and the graph labels.

### PlotFreqGraph.m

```

1 function PlotFreqGraph(f, atten1, atten2, phase1, phase2, ...
      velocity1, velocity2, label1, label2)
2
3 %Plot Frequency Graphs
4
5 %Attenuation Plot
6 figure(2)
7 set(gca,'FontSize',16,'fontWeight','bold');
8 set(gcf,'color',[1 1 1]);
9 loglog((f(1:512)), abs(atten1(1:512)), '-b', (f(1:512)), ...
      abs(atten2(1:512)), ':r','LineWidth',1.25)
10 xlabel('Frequency (Hz)')
11 ylabel('Attenuation (dB/m)')
12 h2 = legend (label1,label2);
13 set(h2, 'Location','NorthWest');
14 axis([106 4*107 10-3 101]);
15
16 %Phase Constant Plot

```

```

17 figure(3)
18 set(gca,'FontSize',16,'fontWeight','bold');
19 set(gcf,'color',[1 1 1]);
20 loglog((f(1:512)), abs(phase1(1:512)), '-b', (f(1:512)), ...
        abs(phase2(1:512)), ':r','LineWidth',1.25)
21 xlabel('Frequency (Hz)')
22 ylabel('Phase Constant (rad/m)')
23 h4 = legend (label1,label2);
24 set(h4, 'Location','NorthWest')
25 axis([10^6 4*10^7 10^-4 10^1])
26
27 %Propagation Velocity Plot
28 figure(4)
29 set(gca,'FontSize',16,'fontWeight','bold');
30 set(gcf,'color',[1 1 1]);
31 loglog((f(1:512)), abs(velocity1(1:512)), '-b', (f(1:512)), ...
        abs(velocity2(1:512)), ':r','LineWidth',1.25)
32 xlabel('Frequency (Hz)')
33 ylabel('Propagation Velocity (m/s)')
34 h5 = legend (label1,label2);
35 set(h5, 'Location','NorthWest')
36 axis([10^6 4*10^7 10^6 10^10])
37
38
39 end

```

The PlotFreqGraph.m code plots three figures; attenuation plot, phase constant plot and propagation velocity plot. All three plots have a frequency range of 1 to 30 MHz. Each plot will have two sets of values being compared, which is determined by the variables inputted to the function. The input for the function are: the frequency, two attenuation vectors, two phase constant vectors, two propagation velocity vectors, and the graph labels.

## A.2.2 Code Implementation

The variations in the implementation of the code were due to the type of test that was being analysed. Below are the three main files used to complete the analysis of each test. The different sections in the code will be described using the Matlab comment delimiter, %.

### SemiconductorComparison.m

```
1 %Comparison Between Power Cable With and Without Outer ...  
   Semiconducting Layer  
2  
3 clc  
4 clear all  
5  
6 %Input into Vectors  
7  
8 reflectFull1 = ...  
9 xlsread(...  
10 'WithSemicon/7Jan200nsGenminLab3/Newfile2max.xlsx',...  
11 'B3:B14002');  
12 reflectFull2 = ...  
13 xlsread(...  
14 'WithoutSemicon/9Jan200nsGenminLab2/Newfile2max.xlsx',...  
15 'B3:B14002');  
16  
17 %Power Cable with Semicon  
18 incid1 = ...  
19 xlsread(...  
20 'WithSemicon/7Jan200nsGenminLab3/Newfile2max3.xlsx',...  
21 'B1:B10000');  
22 reflect1= ...  
23 xlsread(...  
24 'WithSemicon/7Jan200nsGenminLab3/Newfile2max3.xlsx',...  
25 'A1:A10000');  
26  
27 %Power Cable without Semicon  
28 incid2 = ...  
29 xlsread(...  
30 'WithoutSemicon/9Jan200nsGenminLab2/Newfile2max3.xlsx',...
```



```

31 'B1:B10000');
32 reflect2= ...
33 xlsread(...
34 'WithoutSemicon/9Jan200nsGenminLab2/Newfile2max3.xlsx',...
35 'A1:A10000');
36
37 timelength = ...
38 xlsread(...
39 'WithSemicon/7Jan200nsGenminLab/Newfile1max.xlsx',...
40 'A3:A14002');
41
42 increment = 2.00e-10; %time increment
43
44 label1 = 'With Semicon';
45 label2 = 'Without Semicon';
46
47 %Setup Frequency response / Fourier
48
49 Fs = 5e9;
50 F0 = 1e6; %First Sample at 1MHz
51
52 T0 = 1/F0;
53 T = 1/Fs;
54 length1 = 8.25;
55 N0 = T0/T;
56 t = 0:T:T*(N0-1);
57 t=t';
58
59 k = (0:N0-1);
60 k=k';
61 w = 2*pi*k/T0;
62 f = k/T0;
63
64 %Frequency Caluclations - With Semicon
65
66 [atten1, phasel, velocity1] = FreqDomain(incidl, reflect1, ...
        w, length1);
67
68 %Frequency Caluclations - Without Semicon

```

```

69
70 [atten2, phase2, velocity2] = FreqDomain(incid2, reflect2, ...
    w, length1);
71
72 %Attenuation Calculations
73
74 %Calculates the mean, mean difference and percentage ...
    difference between
75 %1 and 7 MHz
76 diffAlpha_1 = atten1(2:8)-(atten2(2:8));
77 AttenMean_1 = mean(diffAlpha_1);
78 Mean_1 = mean(abs(atten1(2:8)));
79 MeanSemi_1 = mean(abs(atten2(2:8)));
80 perc_1 = AttenMean_1/Mean_1*100;
81
82 %Calculates the mean, mean difference and percentage ...
    difference between
83 %7 and 30 MHz
84 diffAlpha_2 = abs(atten1(9:31))-abs(atten2(9:31));
85 AttenMean_2 = mean(diffAlpha_2);
86 Mean_2 = mean(abs(atten1(9:31)));
87 MeanSemi_2 = mean(abs(atten2(9:31)));
88 perc_2 = AttenMean_2/Mean_2*100;
89
90 %Phase Calculations
91
92 %Calculates the mean difference difference between 1 and ...
    20 MHz
93 diffPhase_1 = abs(phase1(2:21)) - abs(phase2(2:21));
94 PhaseMean_1 = mean(diffPhase_1);
95 Phase_1 = mean(abs(phase1(2:21)));
96 PhaseSemi_1 = mean(abs(phase2(2:21)));
97 perc_3 = PhaseMean_1/Phase_1*100;
98
99 %PropVel Calculations
100
101 %Calculates the mean difference difference between 1 and ...
    20 MHz
102 diffVel_1 = abs(velocity2(2:21))-abs(velocity1(2:21));

```

```

103 VelMean_1 = mean(diffVel_1);
104 Vel_1 = mean(abs(velocity1(2:21)));
105 VelSemi_1 = mean(abs(velocity2(2:21)));
106 perc_4 = VelMean_1/Vel_1*100;
107
108 %Plot Graphs
109
110 PlotTimeGraph(reflectFull1, reflectFull2, timelength, ...
    increment, labell1, label2);
111
112 PlotFreqGraph(f, atten1, atten2, phase1, phase2, ...
    velocity1, velocity2, labell1, label2);
113

```

## LengthComparison.m

```

1 %Comparison Between 8.25 m and 20 m Power Cable
2
3 clc
4 clear all
5
6 %Input into Vectors
7
8 reflectFull1 = ...
9 xlsread(...
10 'WithSemicon/7Jan200nsGenminLab3/Newfile2max.xlsx',...
11 'B3:B14002');
12 reflectFull2 = ...
13 xlsread(...
14 '20mCable/16Jan200nsHVLab2/Newfile2max.xlsx',...
15 'B3:B14002');
16
17 %Power Cable - 8.25m
18 incid1 = ...
19 xlsread(...
20 'WithSemicon/7Jan200nsGenminLab3/Newfile2max3.xlsx',...
21 'B3:B10002');
22 reflect1= ...
23 xlsread(...

```

```

24 'WithSemicon/7Jan200nsGenminLab3/Newfile2max3.xlsx',...
25 'A1:A10000');
26
27 %Power Cable - 20m
28 incid2 = ...
29 xlsread(...
30 '20mCable/16Jan200nsHVLab2/Newfile2max3.xlsx',...
31 'B3:B10002');
32 reflect2 = ...
33 xlsread(...
34 '20mCable/16Jan200nsHVLab2/Newfile2max3.xlsx',...
35 'A1:A10000');
36
37 timelength = ...
38 xlsread(...
39 'WithSemicon/7Jan200nsGenminLab/Newfile1max.xlsx',...
40 'A3:A14002');
41
42 increment = 2.00e-10; %time increment
43
44 label1 = '8.25 m';
45 label2 = '20 m';
46
47 %Setup Frequency response / Fourier
48
49 Fs = 5e9;
50 F0 = 1e6; %First Sample at 1MHz
51
52 T0 = 1/F0;
53 T = 1/Fs;
54 length1 = 8.25;
55 N0 = T0/T;
56 t = 0:T:T*(N0-1);
57 t=t';
58
59 k = (0:N0-1);
60 k=k';
61 w = 2*pi*k/T0;
62 f = k/T0;

```

```

63
64 %Frequency Calculations - 8.25 m
65
66 [atten1, phase1, velocity1] = FreqDomain(incid1, reflect1, ...
    w, length1);
67
68 %Frequency Calculations - 20 m
69
70 [atten2, phase2, velocity2] = FreqDomain(incid2, reflect2, ...
    w, length1);
71
72 %Attenuation Calculations
73
74 %Calculates the mean, mean difference and percentage ...
    difference between
75 %1 and 20 MHz
76 diffAlpha_1 = abs(atten1(2:21))-abs(atten2(2:21));
77 AttenMean_1 = mean(diffAlpha_1);
78 Mean_1 = mean(abs(atten1(2:21)));
79 MeanLength_1 = mean(abs(atten2(2:21)));
80 perc_1 = AttenMean_1/Mean_1*100;
81
82 %20 and 30 MHz
83 diffAlpha_2 = abs(atten1(21:31))-abs(atten2(21:31));
84 AttenMean_2 = mean(diffAlpha_2);
85 Mean_2 = mean(abs(atten1(21:31)));
86 MeanLength_2 = mean(abs(atten2(21:31)));
87 perc_1 = AttenMean_2/Mean_2*100;
88
89 %Phase Calculations
90
91 %Calculates the mean difference difference between 1 and ...
    30 MHz
92 diffPhase_1 = abs(phase1(2:31)) - abs(phase2(2:31));
93 PhaseMean_1 = mean(diffPhase_1);
94 Phase_1 = mean(abs(phase1(2:31)));
95 PhaseLength_1 = mean(abs(phase2(2:31)));
96 perc_3 = PhaseMean_1/Phase_1*100;
97

```

```

98 %PropVel Calculations
99
100 %Calculates the mean difference difference between 1 and ...
    30 MHz
101 diffVel_1 = abs(velocity2(2:31))-abs(velocity1(2:31));
102 VelMean_1 = mean(diffVel_1);
103 Vel_1 = mean(abs(velocity1(2:31)));
104 VelLength_1 = mean(abs(velocity2(2:31)));
105 perc_4 = VelMean_1/Vel_1*100;
106
107 %Plot Graphs
108
109 PlotTimeGraph(reflectFull1, reflectFull2, timelength, ...
    increment, label1, label2);
110
111 PlotFreqGraph(f, atten1, atten2, phase1, phase2,...
112             velocity1, velocity2, ...
                label1, label2);

```

## TypeComparison.m

```

1 %Comparison Between Power Cable and RG-58
2
3 clc
4 clear all
5
6 %Input into Vectors
7
8 reflectFull1 = ...
9 xlsread(...
10 'WithSemicon/7Jan200nsGenminLab3/Newfile2max.xlsx',...
11 'B3:B14002');
12
13 reflectFull2 = ...
14 xlsread(...
15 'WithoutSemicon/9Jan200nsGenminLab2/Newfile2max.xlsx',...
16 'B3:B14002');
17

```

```

18 %Power Cable
19 incid1 = ...
20 xlsread(...
21 'WithSemicon/7Jan200nsGenminLab3/Newfile2max3.xlsx',...
22 'B1:B10000');
23 reflect1= ...
24 xlsread(...
25 'WithSemicon/7Jan200nsGenminLab3/Newfile2max3.xlsx',...
26 'A1:A10000');
27
28 %RG-58
29 incid2 = ...
30 xlsread(...
31 'HFCable/21Jan200nsHVLab3/Newfile2max3.xlsx',...
32 'B1:B10000');
33 reflect2 = ...
34 xlsread(...
35 'HFCable/21Jan200nsHVLab3/Newfile2max3.xlsx',...
36 'A1:A10000');
37
38 timelength = ...
39 xlsread(...
40 'WithSemicon/7Jan200nsGenminLab2/Newfile1max.xlsx',...
41 'A3:A14002');
42
43 increment = 2.00e-10; %time increment
44
45 label1 = 'MV Power Cable';
46 label2 = 'RG-58 Cable';
47
48 %Setup Frequency response / Fourier
49
50 Fs = 5e9;
51 F0 = 1e6; %First Sample at 1MHz
52
53 T0 = 1/F0;
54 T = 1/Fs;
55 length1 = 8.25;
56 N0 = T0/T;

```

```

57 t = 0:T:T*(N0-1);
58 t=t';
59
60 k = (0:N0-1);
61 k=k';
62 w = 2*pi*k/T0;
63 f = k/T0;
64
65 %Frequency Caluclations - MV Power Cable
66
67 [atten1, phase1, velocity1] = FreqDomain(incid1, reflect1, ...
    w, length1);
68
69 %Frequency Caluclations - HF Cable
70
71 [atten2, phase2, velocity2] = FreqDomain(incid2, reflect2, ...
    w, length1);
72
73 %Attenuation Calculations
74
75 %Calculates the mean, mean difference and percentage ...
    difference between
76 %1 and 10 MHz
77 diffAlpha_1 = abs(atten1(2:31))-abs(atten2(2:31));
78 AttenMean_1 = mean(diffAlpha_1);
79 Mean_1 = mean(abs(atten1(2:31)));
80 MeanRG_1 = mean(abs(atten2(2:31)));
81 perc_1 = AttenMean_1/Mean_1*100;
82
83 %Calculates the mean, mean difference and percentage ...
    difference between
84 %10 and 20 MHz
85 diffAlpha_2 = abs(atten1(11:21))-abs(atten2(11:21));
86 AttenMean_2 = mean(diffAlpha_2);
87 Mean_2 = mean(abs(atten1(11:21)));
88 MeanRG_2 = mean(abs(atten2(11:21)));
89 perc_2 = AttenMean_2/Mean_2*100;
90
91 %Phase Calculations

```



```

92
93 %Calculates the mean difference difference between 1 and ...
    20 MHz
94 diffPhase_1 = abs(phase1(2:21)) - abs(phase2(2:21));
95 PhaseMean_1 = mean(diffPhase_1);
96 Phase_1 = mean(abs(phase1(2:21)));
97 PhaseSemi_1 = mean(abs(phase2(2:21)));
98 perc_3 = PhaseMean_1/Phase_1*100;
99
100 %PropVel Calculations
101
102 %Calculates the mean difference difference between 1 and ...
    20 MHz
103 diffVel_1 = abs(velocity2(2:21))-abs(velocity1(2:21));
104 VelMean_1 = mean(diffVel_1);
105 Vel_1 = mean(abs(velocity1(2:21)));
106 VelHF_1 = mean(abs(velocity2(2:21)));
107 perc_4 = VelMean_1/Vel_1*100;
108
109 %Plot Graphs
110
111 PlotTimeGraph(reflectFull1, reflectFull2, timelength, ...
    increment, label1, label2);
112
113 PlotFreqGraph(f, atten1, atten2, phase1, phase2,...
114             velocity1, velocity2, ...
    label1, label2);

```